



# Comparative analysis of overexpressed *Fragaria vesca* S-adenosyl-L-methionine synthase (*FvSAMS*) and decarboxylase (*FvSAMDC*) during salt stress in transgenic *Nicotiana benthamiana*

László Kovács<sup>1</sup> · Ákos Mendel<sup>1</sup> · Anna Szentgyörgyi<sup>1</sup> · Sándor Fekete<sup>1</sup> · Ferenc Söre<sup>1</sup> · Katalin Posta<sup>1</sup> · Erzsébet Kiss<sup>1</sup>

Received: 17 May 2019 / Accepted: 3 February 2020 / Published online: 18 February 2020  
© The Author(s) 2020

## Abstract

We investigated the effect of overexpressing *Fragaria vesca* L. cv. Rügen S-adenosyl-L-methionine synthase (*FvSAMS*) and decarboxylase (*FvSAMDC*) genes on control and salt stressed *Nicotiana benthamiana* Domin plants. According to previous studies the overproduction of both proteins enhances the abiotic stress tolerance of plants, but the two enzymes have not yet been studied in one experimental system. We found that the transgenic plants subjected to long-term salt stress displayed higher levels of tolerance than the wild type (WT). In contrast to several earlier studies no antagonistic effect between ethylene and polyamine biosynthesis was observed in our experimental system. Overexpression of *FvSAMDC* had higher impact on the plant physiological parameters both in control and salt stress conditions, than that of *FvSAMS*. Based on the data measured in the *FvSAMDC* lines there appears to be a positive correlation between the free polyamine levels and the proline content as well as the amount of ethylene, while there is a negative correlation between the free polyamine levels and the lignin content in the plants exposed to salt stress. The transformation vectors contained the CaMV35S promoter, the coding sequence of *FvSAMS* and *FvSAMDC* fused with synthetic green fluorescent protein (*sGFP*). We detected the subcellular localization of both enzymes and examined the possible stress induced changes in their distribution. In the case of *FvSAMS::sGFP* nuclear, nucleolar, cytoplasmic (near to the plasmalemma), plastid membrane, whereas in *FvSAMDC::sGFP* nuclear and homogenous cytoplasmic localization was detected. Therefore, SAM is assumed to be produced in situ for numerous biochemical reactions.

**Keywords** Ethylene · Polyamine · Lignin · Fusion protein · Subcellular localization

## Introduction

Different abiotic stresses lead to severe economic losses each year (Mahajan and Tuteja 2005). High salt levels cause ion toxicity (mainly Na<sup>+</sup>), hyperosmotic stress, and secondary stresses (i. e. oxidative damage) (Zhu 2002; Chinnusamy et al. 2006). Both ethylene and polyamines (putrescine, spermidine and spermine) play an important regulatory role in the biotic and abiotic stress responses of plants (Müller

and Munné-Bosch 2015; Romero et al. 2018) and in larger quantities they have a positive effect on the salt tolerance of plants (Jang et al. 2012; Peng et al. 2014; Shen et al. 2014). The antioxidant enzyme activity is growing on the effect of adequate concentration of both ethylene and polyamine, by this way they increase the homeostasis of reactive oxygen species (ROS) and regulate the balance of Na/K, enhancing the adaptation of plants to the salinity environment (Saha et al. 2015; Tao et al. 2015). S-adenosyl-L-methionine (SAM) is a common precursor of polyamine and ethylene biosynthesis. The biosynthesis of ethylene proceeds through the following steps: SAM → 1-aminocyclopropane-1-carboxylic acid (ACC) → ethylene catalyzed by ACC synthase (ACS) and ACC oxidase (ACO) enzymes. At the same time the SAM decarboxylase (SAMDC) converts SAM to decarboxylated SAM, which acts as an aminopropyl group donor in the synthesis of polyamines. Numerous earlier studies reported on the antagonistic effect of ethylene and

**Electronic supplementary material** The online version of this article (<https://doi.org/10.1007/s10725-020-00587-3>) contains supplementary material, which is available to authorized users.

✉ Erzsébet Kiss  
kiss.erszebet@mkk.szie.hu

<sup>1</sup> Institute of Genetics, Microbiology and Biotechnology, Szent István University, Gödöllő, Hungary

polyamine metabolism in response to various biotic and abiotic stresses (Li et al. 2004; Nambeesan et al. 2012; Yu et al. 2016). Therefore, we also set out to study how the ‘SAM flux’ and ‘SAM deficiency’ influenced the ratio of ethylene and polyamine in response to salt stress. S-adenosyl-L-methionine synthase produces S-adenosyl-L-methionine from L-methionine and ATP. SAM is the second most frequently used enzyme substrate after ATP (Cantoni 1975) and can serve as a methyl group source for amino, ribosyl and aminopropyl groups (Fontecave et al. 2004). Furthermore, SAM is needed for the methylation of DNA, RNA, proteins, lipids, lignin, pectin, volatiles, flavonoids, nicotianamine and biotin (Roeder et al. 2009; Gong et al. 2014). Since DNA methylation causes genes to be shut down, SAM is definitely considered to be a gene expression regulator. According to estimates 95% of SAM is used for methylation and only 3–5% is decarboxylated (Merali and Clarkson 2004). SAM is not only the precursor of ethylene and polyamines, but the secondary metabolite lignin, too. Lignin is one of the main metabolic consumers of SAM. In *mto3 Arabidopsis thaliana* genotype a point mutation of the *SAMS3* gene, causing a single amino acid change in the ATP binding domain, is responsible for the *mto3* phenotype. There is no modification either in *SAMS3* expression pattern or in the amount of SAMS protein produced but there is a decrease in SAMS enzyme activity and in the total amount of SAM and lignin content compared to the wild type (WT), providing evidence for the impact of *SAMS3* on lignin biosynthesis (Shen et al. 2002). Several former studies reported an increase in the amount of *SAMS* mRNA in response to salt stress in rose periwinkle, wheat and ginseng (Schröder et al. 1997; Pulla et al. 2009; Kamal et al. 2012). The overexpression of *SAMS* positively influenced the abiotic stress tolerance of tomato, tobacco and *A. thaliana* (Qi et al. 2010; Gong et al. 2014; Guo et al. 2014; Kim et al. 2015; Ma et al. 2017).

*SAMDC* forms a small gene family in *A. thaliana*—the 4 members of which show high similarity to each other (Franceschetti et al. 2001)—and is a strictly regulated enzyme (Hu et al. 2005). The in vivo production of the enzyme can be both transcriptionally and translationally regulated with the latter being directly influenced by polyamines (Pegg 1986; Kusano and Suzuki 2015). *SAMDC* participates in developmental processes, cell differentiation and it is synthesized as a proenzyme, which undergoes an autocatalytic cleavage. *SAMDC* functions as a dimer in mammals containing an alpha and a beta chain. In numerous higher organisms, its autocatalysis and decarboxylation are stimulated by putrescine, but in plants *SAMDC* is highly active in the absence of putrescine as well (Bennett et al. 2002). *SAM* decarboxylase plays a pivotal role in regulating spermidine and spermine biosynthesis in numerous plant species, since the decarboxylated SAM (dcSAM) produced by the *SAMDC* acts as a substrate for both spermidine and spermine synthase (Kusano

et al. 2008). Embryonic lethality was observed in the double mutant of *bud2* and *samdc1*, underlying the fundamental role of *SAMDC* in plant embryogenesis (Ge et al. 2006). The up- and down-regulation of the *SAMDC* showed that the ethylene and polyamine biosynthesis has antagonistic impact on each other in *A. thaliana* (Hu et al. 2006). Furthermore, the overexpression of carnation *SAMDC* resulted in elevated salt stress tolerance in transgenic tobacco plants (Wi et al. 2006) and the NaCl stress increased the amount of *MdSAMDC1* and *AtSAMDC1* mRNA in apple and *A. thaliana* (Urano et al. 2003; Liu et al. 2008). The silencing of *SAMDC* increased salt sensitivity in tobacco, at the same time dcSAM deficiency had a positive effect on the biomass production and stem length of transgenic plants (Mellidou et al. 2016).

Our goal was to elucidate the functions of these two enzymes (FvSAMS and FvSAMDC) both under control and salinity stress conditions, since they have not been investigated simultaneously in one experimental system. Earlier studies investigated the effect of overexpressing *SAMS* or *SAMDC* during abiotic stresses in *Nicotiana tabacum* L., *Solanum lycopersicum* L. and *A. thaliana* (Boerjan et al. 1994; Roy and Wu 2002; Waie and Rajam 2003; Wi et al. 2006, 2014; Cheng et al. 2009; Peremarti et al. 2009; Qi et al. 2010; Gong et al. 2014; Kim et al. 2015; Ma et al. 2017). Studying concomitant activity of the two enzymes in the same experimental system allows the plant physiological parameters investigated to be related to one another quantitatively, making it possible to build a clearer picture with regard to the role of the two enzymes in salt stress response. In addition, we planned to study the subcellular localization of *FvSAMS::sGFP*, *FvSAMDC::sGFP* and the possible changes in response to 10 mM NaCl stress. The *SAMS* is considered an enzyme with cytosolic localization in plants (Schröder et al. 1997; Ravel et al. 1998; Hanson and Roje 2001), whereas it was found to show nucleocytoplasmic distribution in mammals (Reytor et al. 2009). Furthermore, in earlier studies *SAMDC* activity was found in the chloroplasts, mitochondria and cytosol of plants (Yamanoha and Cohen 1985; Torrigiani et al. 1986), while only cytoplasmic localization was detected in animals (Gritli-Linde et al. 1995).

## Material and methods

### Plant material, vector constructs and bioinformatic analysis

For the identification of sequences, the NCBI database was used. The main ORF of FvSAMS (XP\_004288342.1) codes for 394 amino acids and shows 95% similarity with AtSAMS1 (NP\_171751.1), 93% with AtSAMS2

(NP\_192094.1) and 90% with AtSAMS3 (NP\_181225.1). The main ORF of FvSAMDC (XP\_011462957.1) corresponds to 360 amino acids and its similarity is 64% to AtSAMDC1 (NP\_001154585.1), 66% to AtSAMDC2 (NP\_197099.1), 68% to AtSAMDC3 (NP\_001189972.1) and 43% to AtSAMDC4 (NP\_197394.1). The leaf tissue of *Fragaria vesca* L. cv. Rügen was used for the isolation of RNA and cDNA was synthesized by reverse transcription according to the method described below. The cDNA sequences of FvSAMS and FvSAMDC were amplified with the primer pairs designed for the main ORFs and the CaMV35S promoter was amplified with specific primer pairs (Table S2). NetNES 1.1 (La Cour et al. 2004), TargetP 1.1 (Emanuelsson et al. 2007), cNLS Mapper (Kosugi et al. 2009), GPS-SNO 1.0 (Xue et al. 2010), Nucleolar localization sequence Detector (NoD) (Scott et al. 2011) and PHOSIDA (Gnad et al. 2011) applications were used for bioinformatic analysis of the sequences. The cDNA fragments were ligated into pGWB405 (AB294429.1) and the CaMV35S was ligated into pGWB604 (AB543113.1) binary vector according to manufacturer's protocol (Invitrogen™ Gateway®, ThermoFisher Scientific, Waltham, USA). The pGWB405 contained a constitutive CaMV35S promoter and the synthetic green fluorescent protein (*sGFP*) reporter gene while the pGWB604 carried only the *sGFP*. The FvSPDS::*sGFP* construct used for microscopic analysis was built by us using the pGWB405 vector. The insert codes for the spermidine synthase gene isolated from *F. vesca* L. cv. Rügen. FvSPDS::*sGFP* fusion protein showed only cytoplasmic localization and was used as a cytoplasmic control. The FvSAMS-22 and FvSAMS-25 as well as the FvSAMDC-73 and FvSAMDC-76 transgenic lines are referred to hereinafter as FvSAMS and FvSAMDC lines.

### DNA, RNA isolation and cDNA synthesis

The isolation of genomic DNA, plasmid DNA and total RNA was carried out by the CTAB method, PureYield™ Plasmid Miniprep System Kit (Promega, Madison, USA) and the Total RNA Mini Kit (Plant) (Geneaid®, New Taipei City, Taiwan), respectively, according to the manufacturer's protocols. cDNA was synthesized from total RNA by using Oligo (dT)<sub>18</sub> primer according to the protocol of the Revert-Aid First Strand cDNA Synthesis Kit (ThermoFisher Scientific, Waltham, USA), which was used later for the qPCR analysis.

### Agrobacterium mediated plant transformation and transient expression assay

The *Agrobacterium tumefaciens* GV3101 strain was used for transformation of the *Nicotiana benthamiana* plants based on the method described by Clemente

(2006). The *A. tumefaciens* GV3101 strain contained the pGWB405::*FvSAMS*, the pGWB405::*FvSAMDC* and the pGWB604::*CaMV35S* vectors. The same constructions were used for the in vivo infiltration of the 35-day-old *N. benthamiana* plants based on the method described by Li (2011).

### Plant growth conditions

The seeds of two transgenic T<sub>1</sub> lines from each construct (FvSAMS-22, FvSAMS-25 and FvSAMDC-73, FvSAMDC-76) were germinated on MS medium supplemented with 75 µg/ml kanamycin while the wild type *N. benthamiana* seeds on MS medium without antibiotics, respectively. Fourteen days after germination (14 DAG), 32 seedlings were germinated of each transgenic line and wild type were either transferred onto half strength MS medium without antibiotics or onto the same medium supplemented with 0.58 g/l (10 mM) NaCl. The plants and the explants were kept in 16 h light and 8 h dark periods at 23 °C. Samples were collected 85 days after sowing. We investigated the effect of 17.54 g/l (300 mM) NaCl on the survival of *N. benthamiana* leaf discs on same plant growth conditions than in the case of 10 mM NaCl stress. All plant physiology parameters were measured from *N. benthamiana* plant samples grown in control and 10 mM NaCl stress conditions. All photographs were taken with Fuji FinePix S6500fd camera.

### Chlorophyll *a*, *b* and relative chlorophyll content measurements

Chlorophyll *a* and *b* as well as the total chlorophyll contents were measured according to the method published by Porra et al. (1989). The chlorophyll *a* (Ca) and chlorophyll *b* (Cb), as well as the total chlorophyll (Ct = Ca + Cb) contents were determined based on the absorbance measured at 645 nm (Abs.645) and at 663 nm (Abs.663) by using NanoDrop ND-1000 UV/Vis spectrophotometer (NanoDrop Technologies, USA) and calculated according to the formulas: Ca = 0.0127 (Abs.663) – 0.00269 (Abs.645); Cb = 0.0229 (Abs.645) – 0.00468 (Abs.663). ImageJ 1.51j8 software was used for determining the relative chlorophyll content of leaf discs (Schneider et al. 2012). Leaves of wild type *N. benthamiana* were used for calibration between 0 and 100% chlorophyll content (chlorophyll-free and control chlorophyll samples). We calculated the relative chlorophyll content from the measured values of 12 leaf discs.

### Histochemical detection of H<sub>2</sub>O<sub>2</sub> and O<sub>2</sub><sup>-</sup>

The histochemical visualization of H<sub>2</sub>O<sub>2</sub> and O<sub>2</sub><sup>-</sup> was carried out according to the method described by Kumar et al. (2014). The chlorophyll-free leaves were fixed in 60% (v/v) glycerol.

### Determination of H<sub>2</sub>O<sub>2</sub> content

The H<sub>2</sub>O<sub>2</sub> content was determined according to Velikova et al. (2000). The absorbance of the samples was measured at 390 nm by using the WPA Biotech Photometer 1101 (Cambridge, UK). For plotting the standard curve dilutions of 30% (w/w) H<sub>2</sub>O<sub>2</sub> (Sigma-Aldrich, Saint Louis, USA) were used.

### Electrolyte leakage measurement

The electrolyte leakage measurement was carried out according to the method described by Rizhsky et al. (2002). The conductivity of samples was measured by using Radelkis Conductometer Type OK-104 (Budapest, Hungary).

### Determination of proline content

The semi-quantitative determination of proline content was performed by the isatin paper assay of Ábrahám et al. (2010) protocol. L-proline (Sigma-Aldrich, Saint Louis, USA) solutions were used for plotting the standard curve. Photographs were evaluated using ImageJ 1.51j8 software (Schneider et al. 2012).

### Lignin measurement

The lignin content of the shoots was determined by the acetyl bromide method described by Moreira-Vilar et al. (2014). The absorbance of the samples was measured at 280 nm with WPA Biotech Photometer 1101 (Cambridge, UK). The standard curve was plotted using alkali lignin (Sigma-Aldrich, Saint Louis, USA).

### Ethylene analysis

Ethylene release of the leaf discs was measured according to the method described by Langebartels et al. (1991). We put five leaf discs of 9 mm diameter on filter paper soaked in 1 ml 50 mM MES/NaOH (pH 5.6) and 2% (w/v) sucrose solution. We placed the scrolled filter papers into glass tubes covered by silica septum then incubated at 25 °C for 1 h. 1 ml of gas was injected into the Shimadzu GC-14A gas chromatograph (Kyoto, Japan) with the retention time of ethylene being 0.553 s.

### Polyamine analysis

Polyamines analysis was carried out from leaves as described by Németh et al. (2002). 200 mg plant sample was ground in liquid nitrogen, extracted with 2 × 1 ml 0.2 M ice cold perchloric acid, put on ice for 20 min, then centrifuged at 4 °C for 20 min (10,000×g). In the case of

free PA (polyamine) fraction, a dansyl-chloride derivative was prepared from 100 µl supernatant (Smith and Davies 1985). Dansylated polyamines were measured in a WATERS W 2690 (Milford, USA) HPLC instrument using acetonitrile (Sigma-Aldrich, Saint Louis, USA) carrier.

### qPCR analysis

Primers were designed for the sequences of the genes to be examined, the main parameters of which are shown in Table S2. The reactions were performed using Corbett RG-6000 real time PCR equipment (Qiagen, Hilden, Germany). The reaction mixture contained (in 20 µl final volume): 10 µl 2×ABsolute qPCR SYBR Green Mix (ThermoFisher Scientific, Waltham, USA), 1.75 µl/primer (70 nM), 1 µl cDNA (diluted 1/50). For the determination of relative expression levels, the Comparative Quantification method was used supplied as part of Rotor-Gene Q Series Software 2.3.1. (Warton et al. 2004; McCurdy et al. 2008). *N. benthamiana* glyceraldehyde 3-phosphate dehydrogenase (*GAPDH*) gene was used as an endogenous control.

### Microscopic analysis

The detection of *FvSAMS::sGFP*, the *FvSAMDC::sGFP*, the *FvSPDS::sGFP* and the *35S<sub>pro</sub>::sGFP* fusion proteins was performed by Leica TCS SP8 confocal laser scanning microscope and Leica/Leitz DMRB 301-371.010 fluorescence stereo microscope (Leica, Wetzlar, Germany). The leaves were examined without fixation with 1:1 87% (v/v) glycerol:bidistilled water being used for covering. For labelling the endoplasmic reticulum CellLight™ ER-RFP, BacMam 2.0 reagent was used (ThermoFisher Scientific, Waltham, USA). In contrast to the manufacturer's protocol with regard to the cell suspension, the CellLight™ ER-RFP was reinfiltred into the living tissue (100-time dilution) followed by incubation at room temperature for 16 h before the fixation of the tissue [4% (w/v) paraformaldehyde, 0.1% (v/v) Tween 20, 0.1% (v/v) Triton X-100, 0.15 M NaCl, 10 mM sodium phosphate buffer pH 7.5]. The LAS AF Lite 3.3.10134.0 software was applied for the processing of the pictures. ImageJ 1.51j8 software was used for determining the relative fluorescence of sGFP (Schneider et al. 2012).

### Statistical analysis

The results are the mean values of at least three measurements and were statistically evaluated using the standard deviation and ANOVA methods.

## Results

### Short-term salt stress and relative chlorophyll content

We examined the stress response of leaf discs of FvSAMS, FvSAMDC and WT *N. benthamiana* to short-term salt stress (Fig. 1a). We observed that the WT leaf explants died 48 h after being placed on MS medium containing 300 mM NaCl. At the same time, the death of the leaf tissues of FvSAMS and FvSAMDC lines occurred later,

96 h after salt exposure. The relative chlorophyll content of the leaf discs shown in Fig. 1a was quantified and presented in Fig. 1b. Chlorophyll content measured in four sampling times (24, 48, 72 and 96 h after treatment) also supports that there is a difference in the rate of chlorophyll degradation between the leaf discs of WT and transgenic FvSAMS, FvSAMDC lines in response to 300 mM NaCl stress. In the WT leaf explants the chlorophyll content decreased to ~ 15% as early as 48 h after the treatment, while the average value of FvSAMS and FvSAMDC transgenic leaf discs approached this level only in the 96th h.

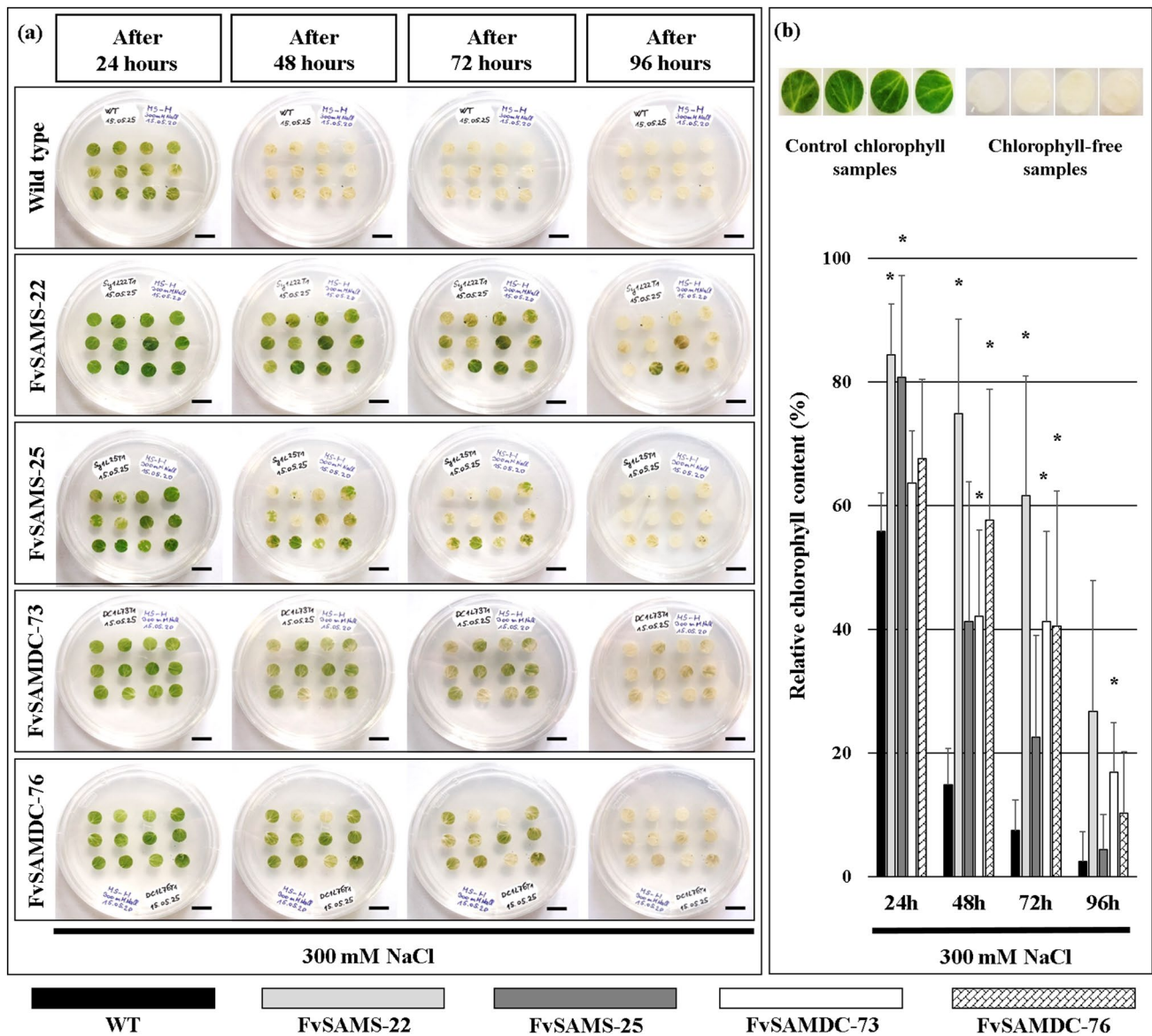


**Fig. 1** Effect of 300 mM NaCl on the survival of *Nicotiana benthamiana* leaf discs. Young leaf discs (from the top to 4th node) were used 50 days after germination. Bars indicate 1 cm (a). Relative chloro-

phyll content of 300 mM NaCl stressed leaf discs, the control chlorophyll and chlorophyll-free samples were used for calibration (b)

## Growth vigour, biomass production and chlorophyll content

The biomass of the plant is a good indication of its response to stress. We observed that both FvSAMS and FvSAMDC lines produced higher shoot biomass and shoot length than the non-transformed ones both in control and 10 mM NaCl stress conditions (Fig. 2a–c).

The chlorophyll content of plants demonstrates their physiological status, therefore we investigated the effect

of long term 10 mM NaCl stress on the total chlorophyll content of transgenic FvSAMS and FvSAMDC lines and wild type plants. The results of chlorophyll *a* and *b* content measurements in Fig. 2d shows that the FvSAMS and FvSAMDC lines contained more chlorophyll than the WT ones both under stress-free and stressed conditions.

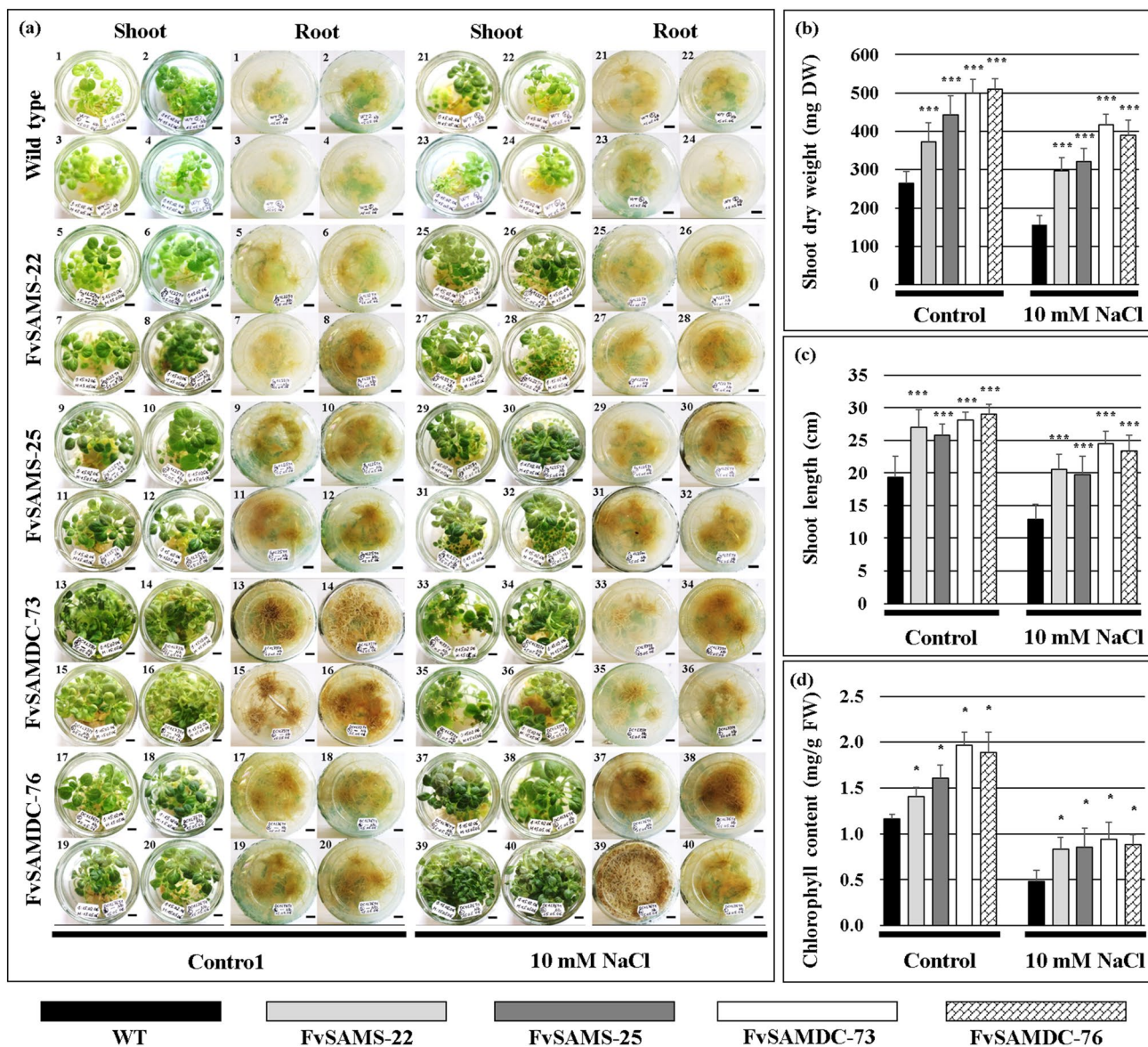


**Fig. 2** Visible effect of overexpression of *FvSAMS* and *FvSAMDC* on shoot and root biomass production in control (1–20) and 10 mM NaCl stress conditions (21–40). The numbers from 1 to 4 and 21 to 24 indicate the wild type, while 5 to 20 and 25 to 40 mark different transgenic lines. The same number refers to the same plant. Bars indicate 1 cm. Photographs were taken 85 days after germination (a).

Dry weight of shoots (b). Results of shoot length measurements (c). Data are the means of six replicates (SD±). Results of chlorophyll *a* and *b* content measurements (d). Data are the means of six (b) twelve (c) and three (d) replicates (SD±), respectively. Three asterisks represent significant differences at  $P < 0.001$  and one asterisk represents significant differences at  $P < 0.05$

### H<sub>2</sub>O<sub>2</sub>, O<sub>2</sub><sup>-</sup> content and electrolyte leakage

The accumulation of ROSs (Reactive Oxygen Species), similarly to that of H<sub>2</sub>O<sub>2</sub> and O<sub>2</sub><sup>-</sup> is in direct proportion with the stress levels of cells, therefore we investigated the H<sub>2</sub>O<sub>2</sub> and O<sub>2</sub><sup>-</sup> contents of tissues by means of histochemical staining as well as quantitative tests. The histochemical staining indicated that the presence of H<sub>2</sub>O<sub>2</sub> could hardly be seen in the stress-free leaves of either the WT or FvSAMS and FvSAMDC lines. More intense coloration of the salt stressed WT leaves corresponds to higher concentrations of H<sub>2</sub>O<sub>2</sub> than in the FvSAMS and FvSAMDC lines (Fig. 3a, left panel). Similarly, to H<sub>2</sub>O<sub>2</sub> more intense coloration appeared in the WT leaves indicating that there is a higher amount of O<sub>2</sub><sup>-</sup> in the non-transformed plants than in the FvSAMS and FvSAMDC lines (Fig. 3a, right panel). Furthermore, salt treated leaves of FvSAMS and FvSAMDC lines showed low H<sub>2</sub>O<sub>2</sub> contents compared to the WTs (Fig. 3b).

The measure of electrolyte leakage gives information about the status of the membranes. Therefore, we examined the electrolyte leakage of the leaf discs both under control

and salt stress conditions (Fig. 3c). We detected lower rates of electrolyte leakage in both FvSAMS and FvSAMDC lines both under control and stress conditions than in the WTs.

### Proline and lignin content

Proline accumulation is also considered to be a good indicator of stress response. There was no change of proline content in control condition. Salt stress increased (4.3 fold) the proline accumulation only in FvSAMDC lines (Fig. 4a).

Lignin is known to accumulate between the primary and secondary cell wall to ensure the strength of cell wall during plant development. A firm cell wall provides the cells with increased protection against biotic and abiotic stresses. We also measured the lignin content of the stem under both control and salt stress conditions (Fig. 4b). Under the control conditions more lignin was found in the shoots of FvSAMS and FvSAMDC lines than in WTs. The salt stress caused a rise in the lignin content of the WT and FvSAMS lines, but a significant decrease was found in the FvSAMDC genotypes.

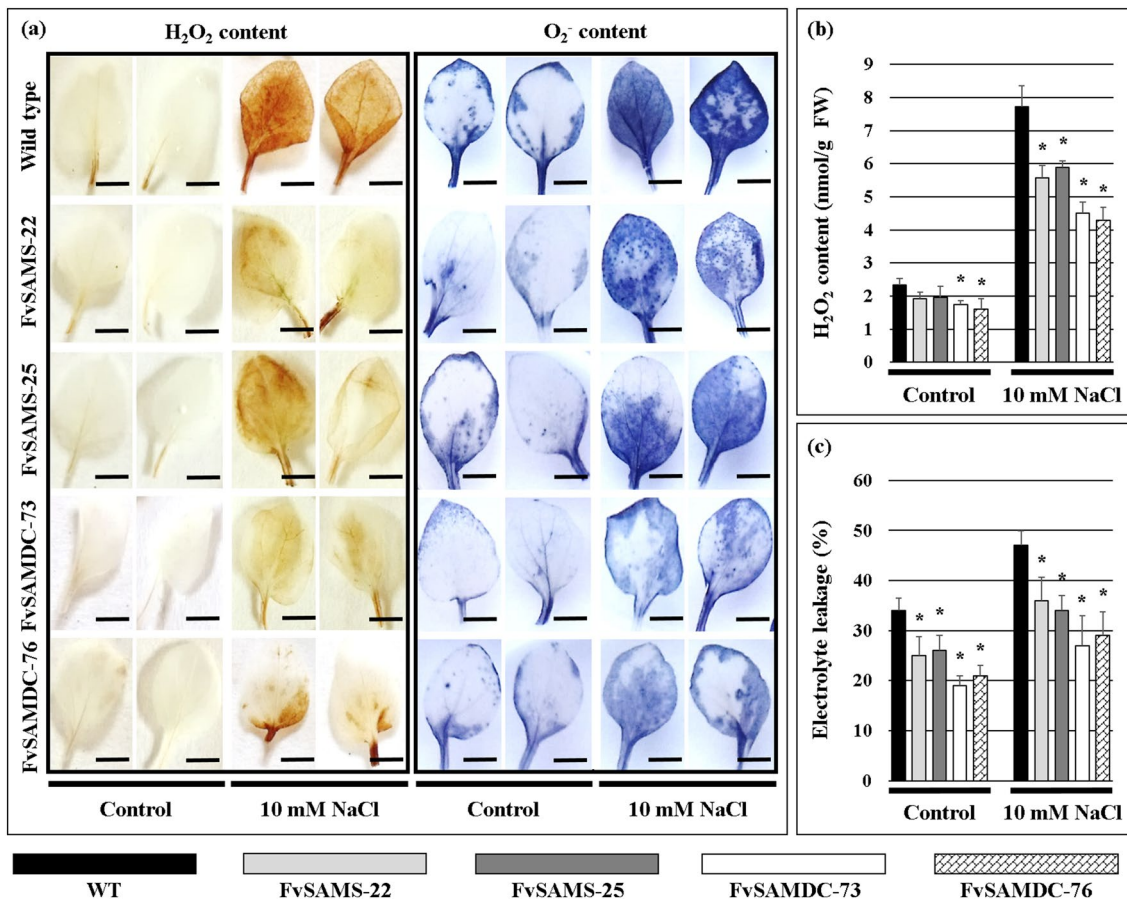


**Fig. 3** Histochemical detection of H<sub>2</sub>O<sub>2</sub> (left) and O<sub>2</sub><sup>-</sup> (right) in *Nicotiana benthamiana* leaves. Bars indicate 1 cm (a). H<sub>2</sub>O<sub>2</sub> content of the leaves (b). Results of electrolyte leakage measurements (c). Data are

the means of three replicates (SD ±). One asterisk represents significant differences at P < 0.05

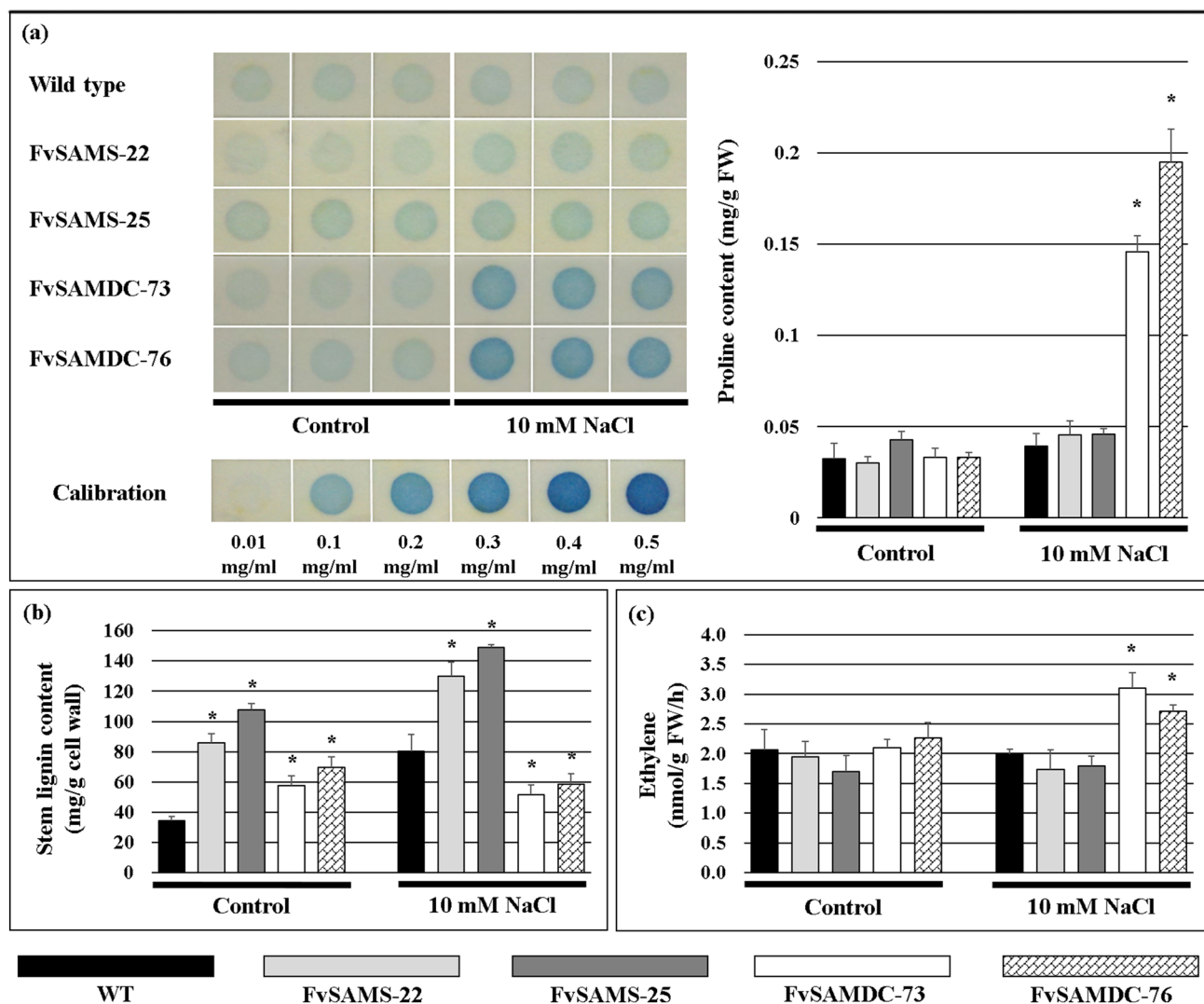


**Fig. 4** Determination of proline content (a). Stem lignin content measurements (b). Ethylene production of leaf discs (c). Data are the means of three replicates (SD  $\pm$ ). One asterisk represents significant differences at  $P < 0.05$

### Ethylene and polyamine content

Since ethylene is implicated in numerous stress responses, we investigated the effect of overproducing *FvSAMS* and *FvSAMDC* on the levels of ethylene both under control and stress conditions. In the FVSAMS lines there was no significant change in ethylene production either in control or salt stress conditions. The FvSAMDC lines did not produce significantly higher levels of ethylene under control conditions, but the salt stress induced a substantial rise in the ethylene production in the *FvSAMDC* transgenic plants than in WT (Fig. 4c).

In addition to ethylene, we examined the free polyamine content of the transgenic *FvSAMS* and *FvSAMDC* lines and WT plants both under control and salinity conditions

(Fig. 5). We detected significantly lower levels of putrescine (Put) in response to stress in the *FvSAMS* lines. However, the amount of Put was found to be significantly higher only in the *FvSAMDC* lines both under the control and stress conditions. In the *FvSAMS* lines significantly higher levels of spermidine (Spd) and spermine (Spm) were only detected in response to stress, while the amount of Spd and Spm was found to be significantly higher both under control and stress conditions in the *FvSAMDC* lines. In the *FvSAMS* lines significantly higher levels of total free polyamine content was only detected in response to stress, while the total free polyamine content was significantly higher in the *FvSAMDC* lines in response to both control and stress conditions.



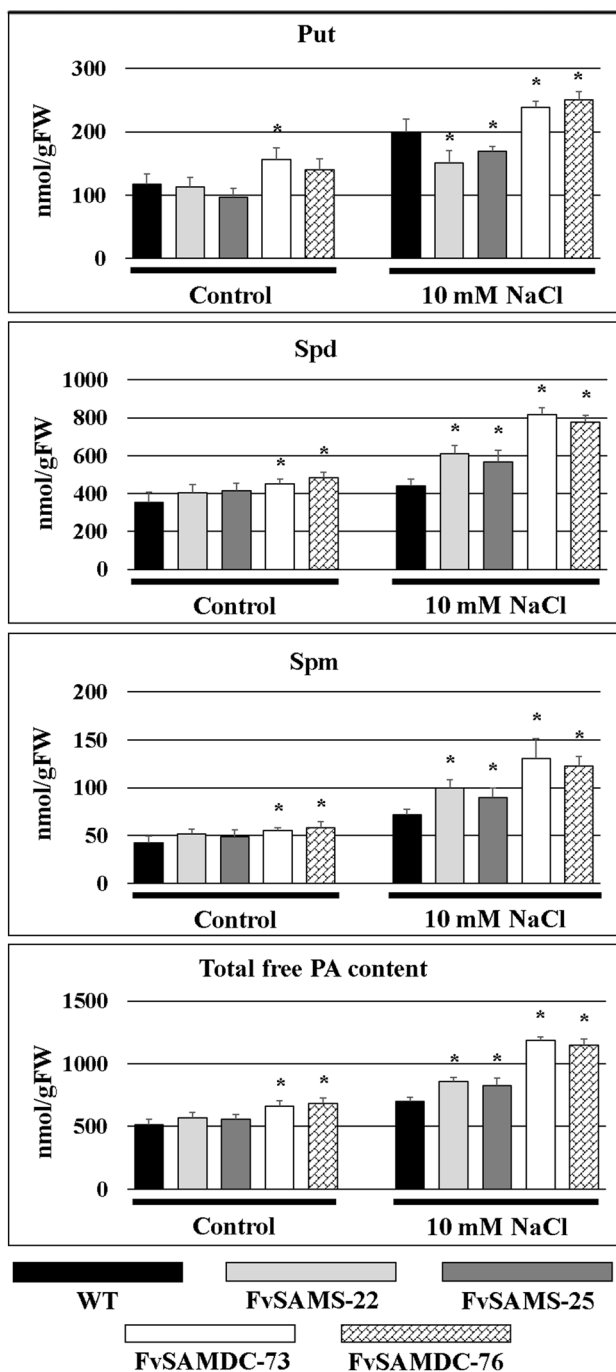


**Fig. 5** Free polyamine (PA) content. Put (putrescine), Spd (spermidine), Spm (spermine). Data are the means of three replicates ( $SD \pm$ ). One asterisk represents significant differences at  $P < 0.05$

### Relative expression measurement

We analyzed the expression of genes participating in ethylene (SAM synthase—*SAMS*; ACC synthase—*ACS*) and polyamine biosynthesis (SAM synthase—*SAMS*; SAM decarboxylase—*SAMDC*; spermidine synthase—*SPDS*; spermine synthase—*SPMS*), the recycling of SAM

(S-adenosyl-L-homocysteine hydrolase—*SAHH*) and the production of two secondary metabolites such as lignin (Cinnamyl-alcohol dehydrogenase—*CAD*) and nicotine (Putrescine N-methyltransferase—*PMT*) (Fig. 6). The relative expression rate of *SAMS*, *SAMDC* and *SAHH* was significantly higher in the Fv*SAMS* and Fv*SAMDC* lines than in the WT's both under control and salt stress conditions. The transcription rate of *ACS* was found to be lower in the Fv*SAMS* lines under non-stressed condition and it was lower in response to salt stress as well. At the same time, Fv*SAMDC* lines displayed higher levels of *ACS* expression than in the WT's under stress condition. The transcription rate of *SPDS* did not show significant difference between the WT's and the Fv*SAMS*, Fv*SAMDC* lines in stress-free environment, while it increased both in the Fv*SAMS* and Fv*SAMDC* lines in response to salt treatment. The relative expression rate of *PMT* was lower in the Fv*SAMS* lines in the control environment and higher in the Fv*SAMDC* lines than in the WT's. Significantly higher rate of *PMT* expression was measured in response to stress in both the Fv*SAMS* and Fv*SAMDC* lines. The expression levels of *CAD* were higher in almost all transgenic lines in control condition and all transgenics under salt stress than in the WT's.

The summary of the measurements in control and 10 mM NaCl stress conditions is shown in Table S1.

### Subcellular localization of Fv*SAMS*::sGFP and Fv*SAMDC*::sGFP

We carried out transient expression investigations with the Fv*SAMS*::sGFP, Fv*SAMDC*::sGFP, Fv*SPDS*::sGFP (*F. vesca* L. cv. Rügen spermidine synthase) and  $35S_{pro}$ ::sGFP constructs. Transient expression of Fv*SAMS*::sGFP, Fv*SAMDC*::sGFP and  $35S_{pro}$ ::sGFP fusion proteins displayed nuclear and cytoplasmic localization, while Fv*SPDS*::sGFP showed only cytoplasmic distribution in epidermal cells (Fig. 7). We noticed that each of the three fusion proteins (Fv*SAMS*::sGFP, Fv*SAMDC*::sGFP and  $35S_{pro}$ ::sGFP) showed endoplasmic reticulum (ER) signals during their transient expression (Fig. S1), therefore we used ER labelling with the application of CellLight™ ER-RFP (Fig. S2). The Fv*SAMS*::sGFP and Fv*SAMDC*::sGFP showed weaker ER signals than the  $35S_{pro}$ ::sGFP construct. The fixation of the leaf tissue was carried out following the ER labelling, which resulted in the sGFP signal becoming less pronounced and therefore allowed us to observe the distinctive nuclear and nucleolar signals of Fv*SAMS*::sGFP, which were detectable in the stable transformants as well (Fig. 8a, b). In the stable transformants, the Fv*SAMS*::sGFP did not show homogeneous cytoplasmic distribution, but it accumulated in the outermost regions of the cytoplasm near the plasmalemma and plastid membrane in palisade parenchyma cells as it is visible in Fig. 8c and d. The distribution

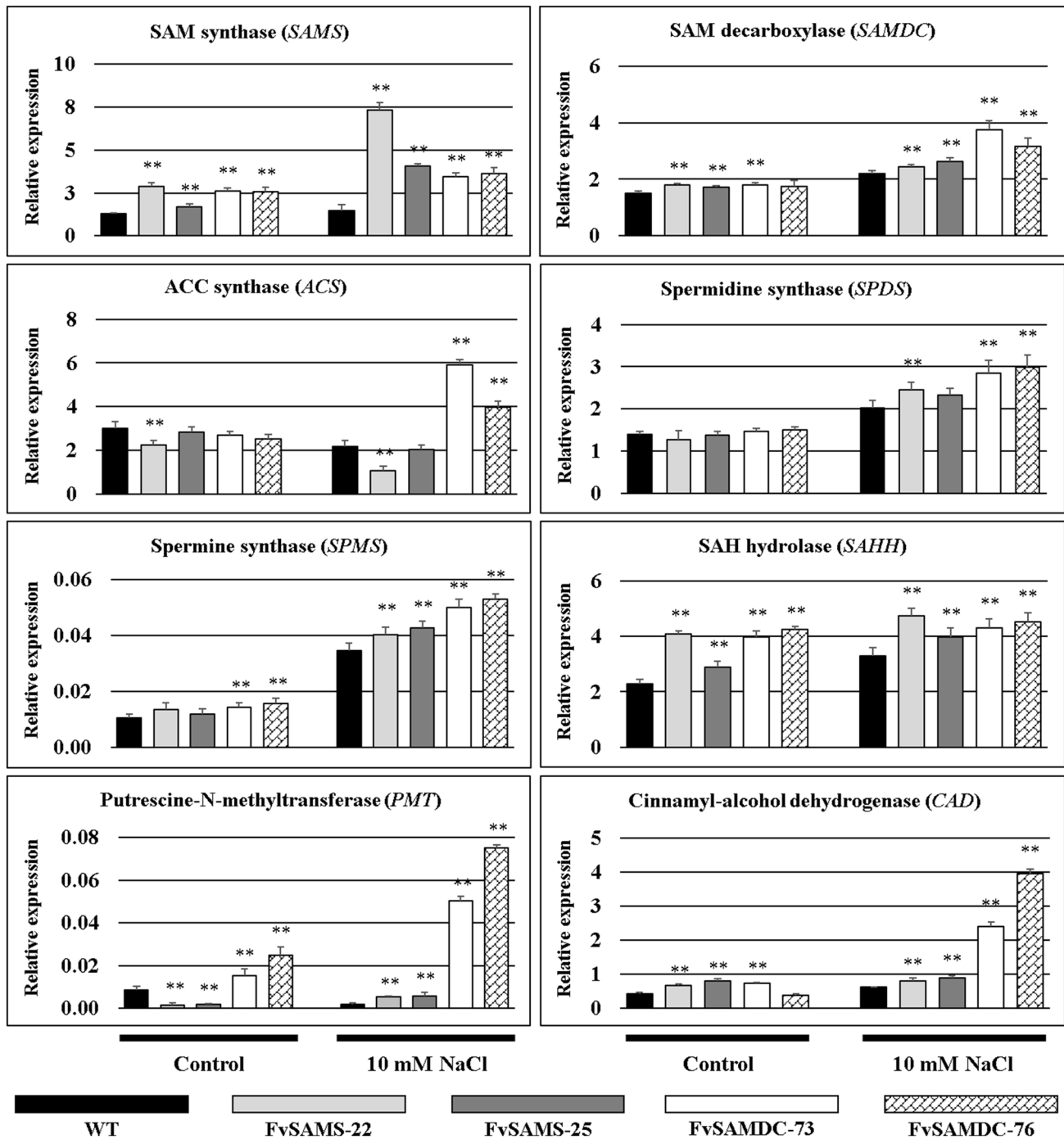


**Fig. 6** Relative expression measurements with qPCR. SAM: S-adenosyl-L-methionine, ACC: 1-aminocyclopropane-1-carboxylic acid, SAH: S-adenosyl-L-homocystein. Data are the means of four replicates (SD  $\pm$ ). Two asterisks represent significant differences at  $P < 0.01$

of *FvSAMS::sGFP* and *FvSAMDC::sGFP* fusion proteins in the stable transformants both under control and saline conditions is illustrated in Fig. 9a. We observed differences in the ratios of nuclear to cytoplasmic distribution under stress-free and stressed conditions. The nuclear signal of *FvSAMS::sGFP* was more intense in the control environment, and the cytoplasmic expression became stronger in

response to salt stress (Fig. 9b, upper part). In the case of *FvSAMDC::sGFP* the amount of fusion proteins increased substantially in response to salt stress both in the nucleus and the cytoplasm (Fig. 9b, lower part). At the same time it could be observed that the *FvSAMDC::sGFP* showed distinctive nuclear, cytoplasmic and nuclear-cytoplasmic localization concurrently (Fig. 10a). We also noticed that in the case of

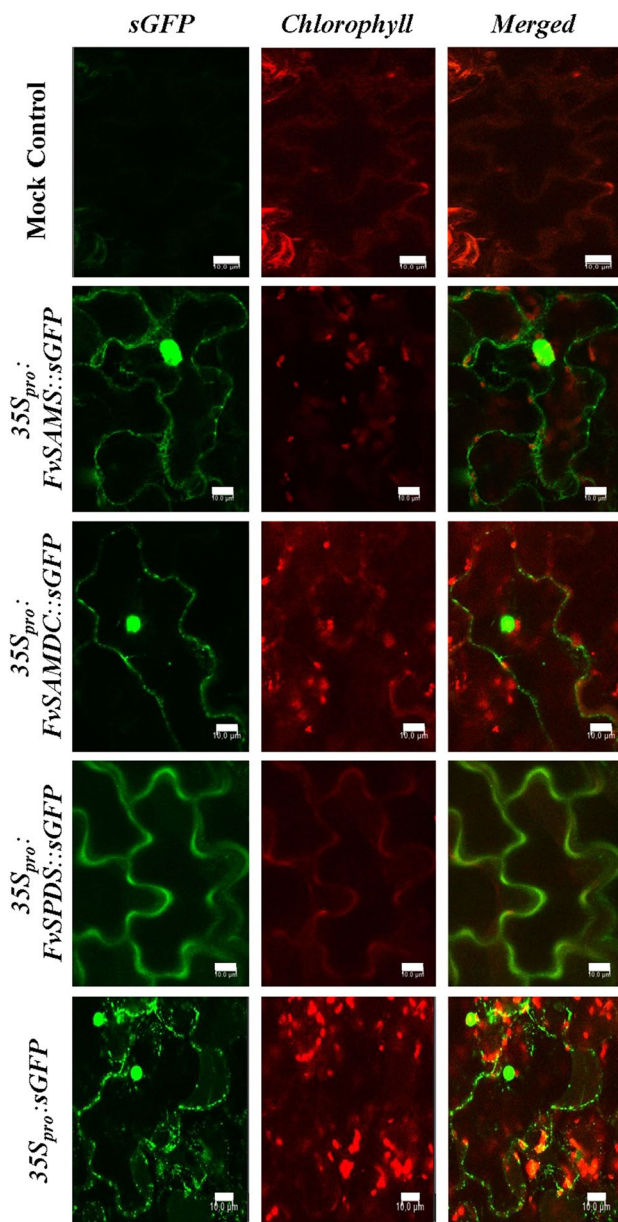


**Fig. 7** Transient expression analysis of *FvSAMS::sGFP*, *FvSAMDC::sGFP*, *FvSPDS::sGFP* and *35S<sub>pro</sub>::sGFP* in epidermal cells. Bars indicate 10  $\mu$ m

*FvSAMS* lines the abundance of the *FvSAMS::sGFP* fusion protein changed depending on the position of the leaves in the plant. In the leaves closest to the apex the *sGFP* protein could be detected in almost all of their cells while moving downwards the number of *sGFP* expressing cells decreased, finally leaving only the guard cells of the stomata giving off the *sGFP* signal (Fig. 10b, ci, ii). Therefore, we determined the amount of *sGFP* mRNA in the leaves from the top to 4th node and from the 5th to 7th nodes in the *FvSAMS* lines. Despite the fact that the detectability of *sGFP* protein was higher in the upper leaves the amount of mRNA showed the

opposite trend with the lower leaves containing ~2–5-times more mRNA than the upper ones (Fig. 10d). Similar phenomenon was not observed in the *FvSAMDC* lines.

### Bioinformatic analysis

To further investigate the nuclear, nucleolar and cytoplasmic (near to the plasmalemma), plastid membrane localization of *FvSAMS::sGFP* and the nuclear, homogenous cytoplasmic localization of *FvSAMDC::sGFP*, the amino acid of *FvSAMS* and *FvSAMDC* sequences were examined by means of various bioinformatic applications. We searched for nuclear localization signals (NLSs), the nuclear export signals (NESs), the nucleolar localization signals (NoLSs) and potential post-translational modification sites in these sequences. Figure 11a shows the absence of a cysteine residue in the enzyme SAMS, which plays an important role in the inhibition of the SAMS by S-nitrosylation. Furthermore, Fig. 11b shows the recognition sequence involved in the inhibition of enzyme SAMS by Protein kinase C. Both *FvSAMS* and *FvSAMDC* contain putative bipartite nuclear localization signal and nuclear export signal sequences, but *FvSAMS* contained no predicted nucleolar localization signals. The predicted post-translational modification sites of *FvSAMS* include Ser-38 and Thr-112 for phosphorylation, Lys-335, 360 and 364 for acetylation, Cys-20 and 31 for S-nitrosylation, Lys-39 and 334 for SUMOylation. Potential sites of post-translational modifications of *FvSAMDC* based on Ser-25, 37, 39, 203, 204, 212, 316 and 317 for phosphorylation, Lys-199 for acetylation, Cys-312 for S-nitrosylation and Lys-334 for SUMOylation (Fig. 11c, d).

### Discussion

In the present study we performed a comparative investigation in an attempt to find out how the overexpression of *FvSAMS* and *FvSAMDC* affects the various physiological parameters of the plants in response to salt stress. We found that the overproduction of *FvSAMS* and *FvSAMDC* decreased chlorophyll degradation in 300 mM NaCl stress (Fig. 1) and increased the biomass in response to 10 mM NaCl stress (Fig. 2), in agreement with earlier findings by others (Roy and Wu 2002; Wi et al. 2006; Qi et al. 2010; Gong et al. 2014; Kim et al. 2015; Ma et al. 2017). However, we found significant differences in the above mentioned parameters even under control conditions compared to the WT plants.

The chloroplasts are the main sites of the production of ROS, including superoxide anions, hydrogen peroxide, hydroxyl radical and singlet oxygen (Mignolet-Spruyt et al. 2016). ROS homeostasis is altered in response to stress. When present at high concentrations, ROS can damage the

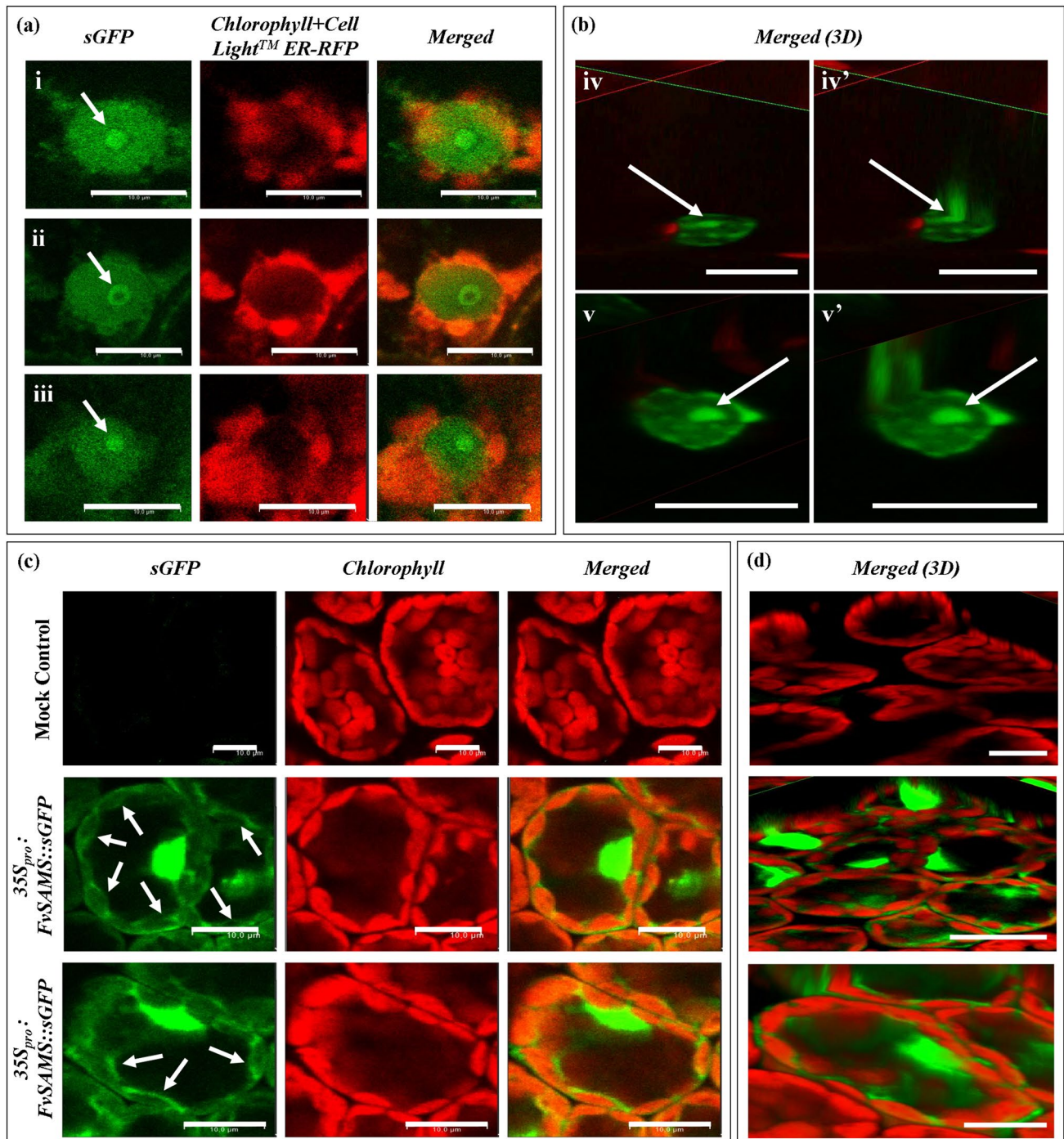


**Fig. 8** *FvSAMS::sGFP* signals in the cell nucleus and nucleolus of epidermal cells with transient expression (a) and in the palisade parenchyma cells of the stable transformant plants in 3D (b). The cytoplasmic (near to the plasmalemma) and plastid membrane localization of *FvSAMS::sGFP* in palisade parenchyma cells (c)

and these *sGFP* signals in 3D (d). The iv–iv' and v–v' refer to the same nucleus. Bars indicate 10  $\mu m$  (a, c, d) and 20  $\mu m$  (b). Arrows indicate plastid membrane (a) and nucleolus (c, d) localization of *FvSAMS::sGFP*

cell and at low concentrations they act as signals in recognising stress and triggering a response. Excessive accumulation of ROS causes oxidative stress, which leads to lipid peroxidation and membrane structure damage, leading

eventually to cell death (Biswas and Mano 2015). Increased membrane stability accounts for significantly lower rates of electrolyte leakage and  $H_2O_2$ ,  $O_2^-$  in both *FvSAMS* and *FvSAMDC* lines both under control and stress conditions than

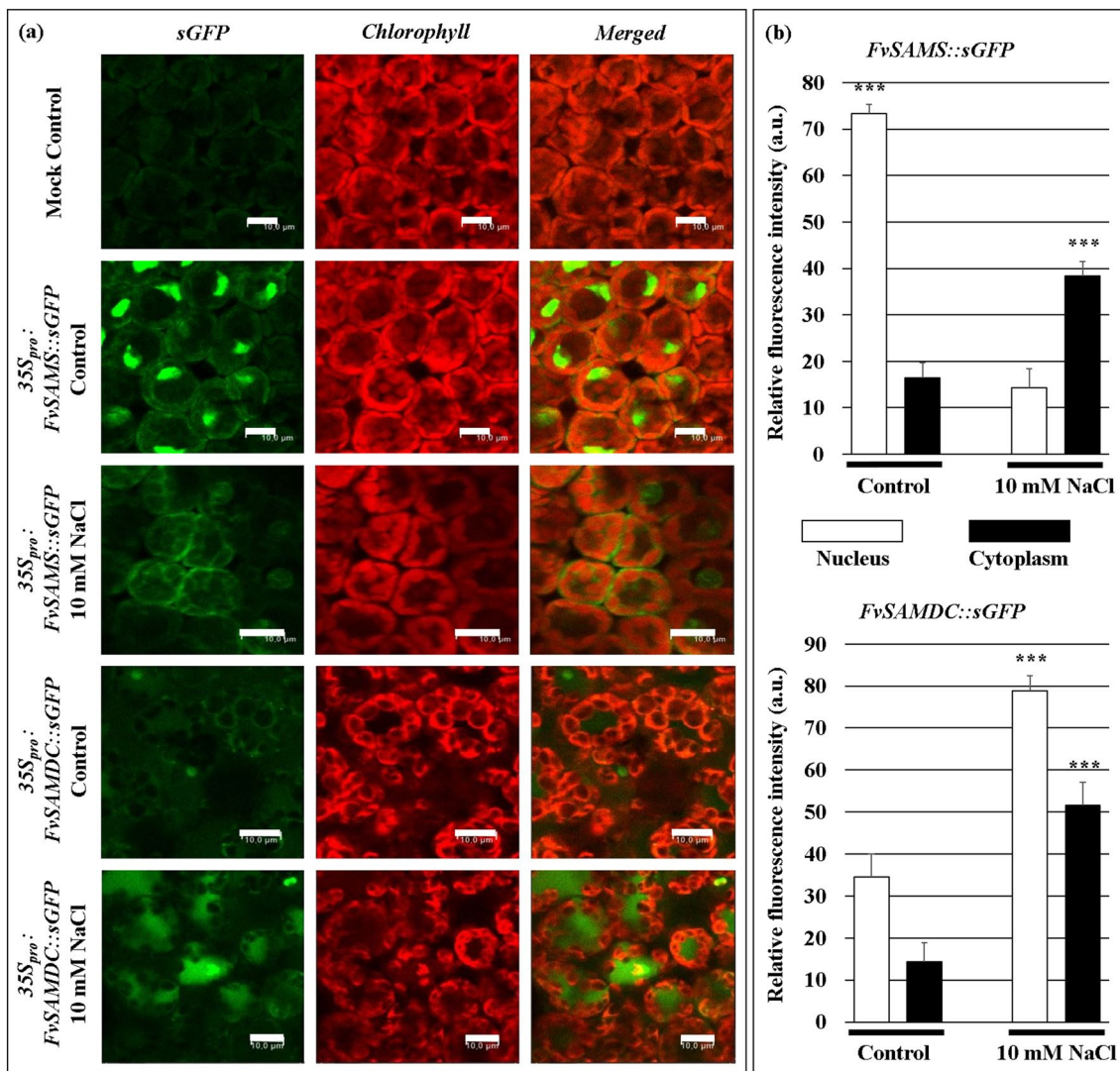


**Fig. 9** Subcellular localization of *FvSAMS::sGFP* and *FvSAMDC::sGFP* in palisade parenchyma cells of stable transformants in control and salt stress conditions. Bars indicate 10  $\mu m$  (a). Relative fluorescence intensity of *FvSAMS::sGFP* and

*FvSAMDC::sGFP* fusion protein in the nucleus and cytoplasm under control and salinity conditions (a. u.: arbitrary unit). Data are the means of ten replicates (SD $\pm$ ). Three asterisks represent significant differences at P < 0.001 (b)

in the WT (Fig. 3). Lower electrolyte loss was measured in *SISAMS*, *MfSAMS1* overproducing tomato and tobacco plants in salt stress conditions (Gong et al. 2014; Guo et al. 2014) and in heat-stressed tomato plants overexpressing yeast *SAMDC* (Cheng et al. 2009) than in the wild types. Significantly lower levels of ROS accumulation could be detected in *SISAMS* and *BvM14-SAMS2* overproducing tomato, *A. thaliana* (Gong et al. 2014; Ma et al. 2017) and in *CaSAMDC* overexpressing *A. thaliana* plants (Wi et al. 2014). Several previous publications reported that the overproduction of *SAMS* and *SAMDC* increased the activity of the ROS scavenging enzymes through increased polyamine biosynthesis (Wi et al. 2006, 2014; Gong et al. 2014; Guo et al. 2014; Ma et al. 2017). There are two biochemical

pathways by which polyamines can exert their control over the homeostasis of ROS. One of the pathways leads to the inhibition of the auto-oxidation of metals, which decreases the electron supply required for the generation of ROS (Shi et al. 2010). The other pathway directly increases the activity of enzymes in the antioxidant system (Shi et al. 2010; Mostofa et al. 2014), which presumably leads to the reduced quantity of  $H_2O_2$  and  $O_2^-$  in the transgenic *FvSAMS* and *FvSAMDC* lines.

Besides the ROS, the amount of accumulating proline in the cell is also a good indicator of the level of stress the plants are exposed to. The elevated proline levels have numerous positive impacts on the abiotic stress tolerance of plants, with proline accumulation being directly proportional

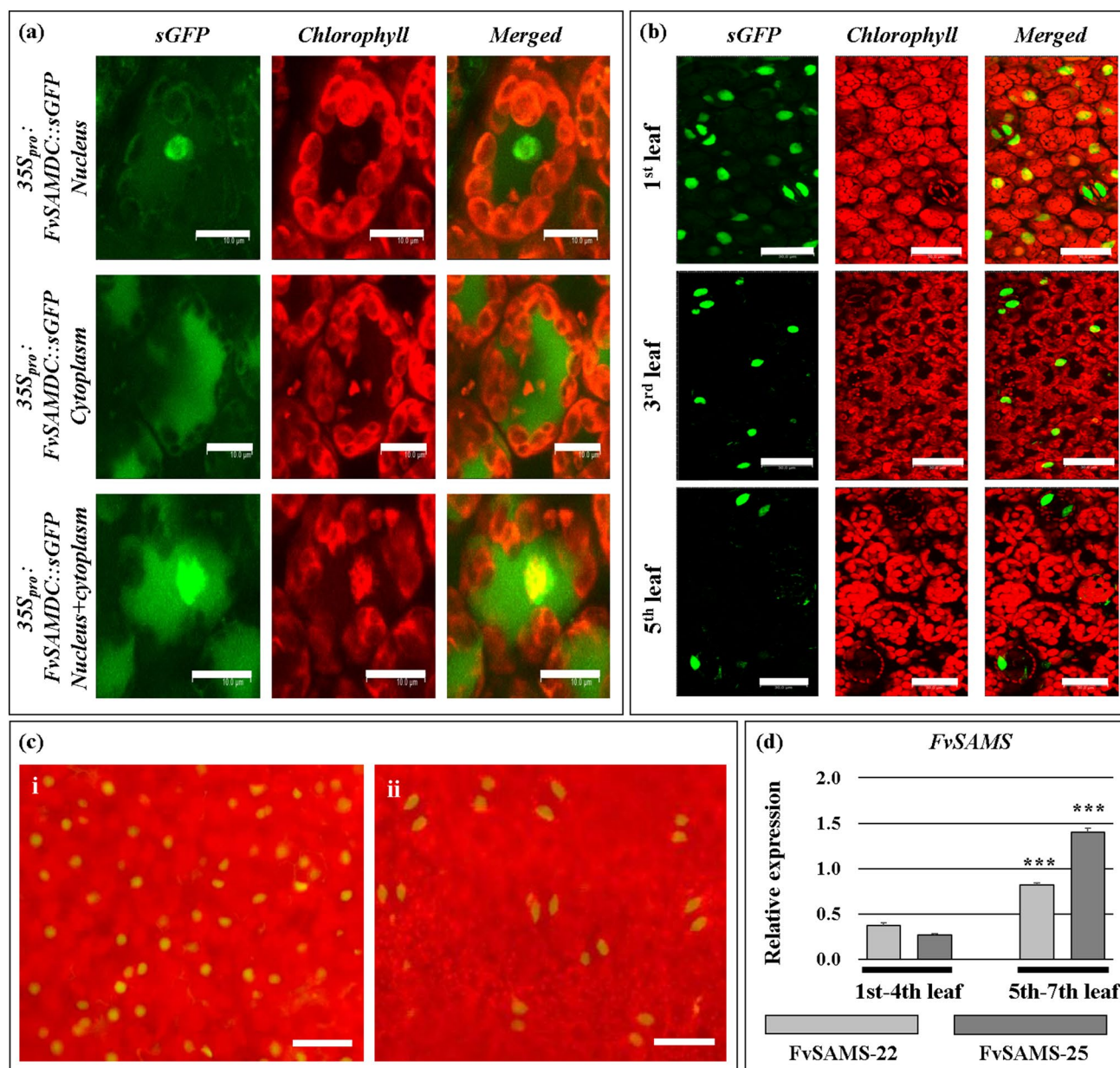


**Fig. 10** Different subcellular localization of *FvSAMDC::sGFP* in palisade parenchyma cells. Bars indicate 10 μm (a). Detection of *FvSAMDC::sGFP* expression in different leaf levels. Bars indicate 30 μm (b). Detecting the expression of *FvSAMDC::sGFP* protein in the stomata in the 1<sup>st</sup> (i) to 5<sup>th</sup> (ii) leaves from above (c). Relative

expression of *FvSAMS* from leaves at different levels. Data are means of four replicates (SD ±). Three asterisks represent significant differences at  $P < 0.001$  (d)

to the levels of polyamines, in spite of the fact that they share a common precursor (glutamic acid) (Simon-Sarkadi et al. 2006; Wen et al. 2011; Cvikrová et al. 2012). Higher levels of total polyamine measured in our *FvSAMS*-expressing lines showed no positive correlations with the proline content detected. In contrast to our results, higher proline levels were found in *A. thaliana* plants overproducing *BvM14-SAMS2* in response to salt stress than in WT plants. The overexpression of *FvSAMDC* increased the levels of proline

in response to salt stress (Fig. 4a), which is in agreement with the higher levels of total polyamine measured in *FvSAMDC* lines.

Since lignin is one of the main metabolic consumers of SAM, we investigated how ‘SAM flux’ and ‘SAM deficiency’ influence the lignin content of plants under control conditions and in response to salt stress. Lignin is deposited between the primary and secondary cell walls during plant development and thereby increases the strength of the stem,

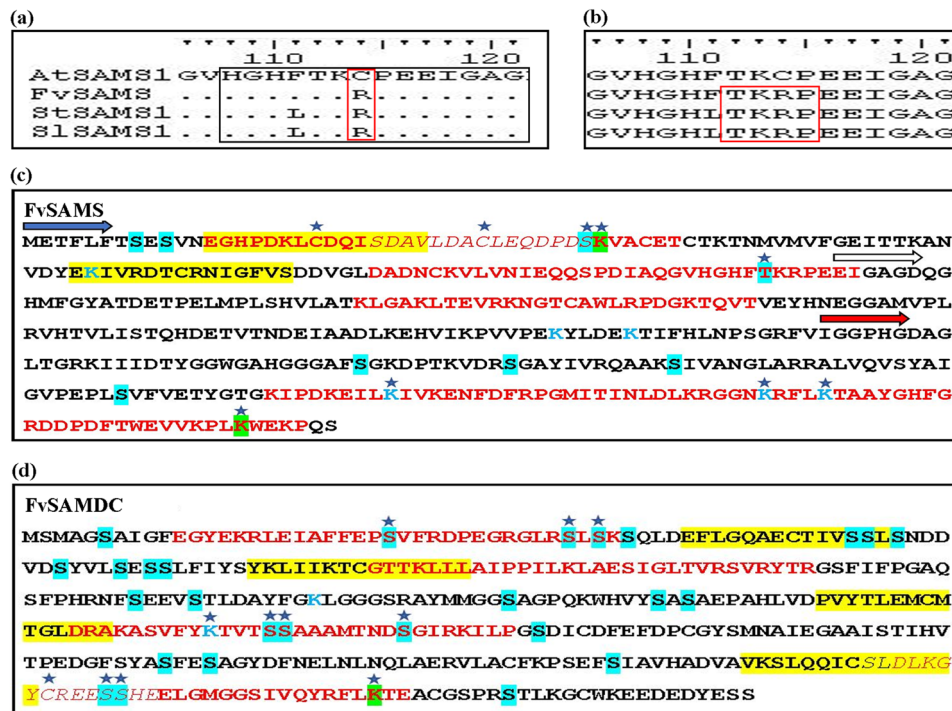


**Fig. 11** Bioinformatic analysis of FvSAMS and FvSAMDC. S-nitrosylation region of AtSAMS1 (NP\_171751.1) proteins (black rectangular) and the lack of cystein (C) necessary for S-nitrosylation in FvSAMS (XP\_004288342.1), SISAMS1 (NP\_001234425.1) and StSAMS1 (NP\_001275609.1) (red rectangle). Dots mark amino acids identical to the sequence of AtSAMS1 (a). Predicted phosphorylation site of Thr-112 and the possible recognition sequence of Protein kinase C (red rectangle) (b). Bioinformatic analysis of the FvSAMS (c) and FvSAMDC (d) amino acid sequences. Colour code: pre-

dicted bipartite NLS (nuclear localization signal) (red letters), predicted S-nitrosylation Sites (highlighted in yellow, in areas of overlap not bold italics), predicted Phosphorylation Sites (highlighted in turquoise), predicted Acetylation Sites (blue letters), predicted SUMOylation (highlighted in green), overlap between predicted NLSs and the post-translational modification sites (star). In the case of FvSAMS the N— (blue arrow), Central-(white arrow) and the C-terminal domains (red arrow) are indicated according to the UniProtKB—Q96551

which, in turn, improves the tolerance of plants against biotic and abiotic stresses. Accelerated lignification was observed in the roots of water-deficient sorghum, salt stressed soybean and salt stressed maize plants (Azaizeh and Steudle 1991; Cruz et al. 1992; Neves et al. 2010). Sánchez-Aguayo et al. (2004) concluded that the elevated activity of SAM in salt stressed tomato plants is commensurate with the increased amount of lignin deposited in vascular tissues. According to our result, both ‘SAM flux’ and ‘SAM deficiency’ increased the rate of lignification in the transgenic FvSAMS and FvSAMDC lines under control conditions. However, in response to salt stress ‘SAM deficiency’ substantially reduced, while ‘SAM flux’ substantially increased lignification, which could have directly increased the tolerance of FvSAMS lines against salt stress (Fig. 4b).

Since SAM is a precursor molecule of ethylene biosynthesis, we also investigated how the overexpression of FvSAMS and FvSAMDC influenced the amount of ethylene under control and stress conditions. Although the overproduction of FvSAMS had no influence on the release of ethylene, the overexpression of FvSAMDC upregulated ethylene

production under stress conditions (Fig. 4c). In previous studies, down-regulated tobacco SAMDC activity did not cause any changes in ethylene production (Torrighiani et al. 2005), while the overexpression of AtSAMDC in A. thaliana plants reduced the amount of ethylene (Hu et al. 2006). Furthermore, neither the overexpression of FvSAMS, nor that of MfSAMS1 in tobacco plants resulted in any significant changes in the amount of ethylene produced (Guo et al. 2014), similarly to our results. However, the overexpression of SAMS increased the level of ethylene production in tomato and A. thaliana plants (Gong et al. 2014; Kim et al. 2015).

Polyamines are known to play an important role in osmotic regulations, membrane stability, and the removal of free radicals under abiotic stresses (Liu et al. 2007; Romero et al. 2018). In accordance with earlier studies, the overexpression of both FvSAMS and FvSAMDC was found to increase the total polyamine levels in response to stress (Roy and Wu 2002; Waie and Rajam 2003; Wi et al. 2006, 2014; Cheng et al. 2009; Peremarti et al. 2009; Gong et al. 2014; Ma et al. 2017). However, the overproduction of the FvSAMDC increased the total polyamine levels more

substantially, while the “SAM surplus” caused a lesser degree of accumulation in the FvSAMS lines (Fig. 5). It follows therefore that in contrast to several earlier studies (Li et al. 2004; Nambesan et al. 2012; Yu et al. 2016), no antagonistic effect between ethylene and polyamine biosynthesis was observed in our experimental system.

Based on the data measured in the FvSAMDC lines there appears to be a positive correlation between the free PA levels and the proline content as well as the amount of ethylene, while there is a negative correlation between the free PA levels and the lignin content when the plants are exposed to salt stress (Figs. 4c, 5).

The overexpression of *FvSAMS* and *FvSAMDC* increased the relative expression rates of genes *SAMS*, *SAMDC*, *SPDS*, *SPMS*, *SAHH*, *PMT* and *CAD* under stress condition (Fig. 6). However, the expression rates of *ACS* decreased in the FvSAMS but increased in the FvSAMDC lines under stress conditions, which was also supported by the ethylene production (Figs. 4c, 6). The relatively high levels of expression of *CAD* in response to stress in the FvSAMDC lines showed no positive correlation with lignin contents (Figs. 4b, 6), according to our assumption the lower lignin content measured in the FvSAMDC lines can induce the higher *CAD* expression in the case of salt stress in order to increase the lignin production. In earlier reports the overexpression of *SAMS* increased the relative expression rates of the genes *SAMS*, *SAMDC*, *ACS*, *SPDS* and *SPMS* in tomato, *Medicago sativa* and *A. thaliana* (Gong et al. 2014; Guo et al. 2014; Kim et al. 2015) and the overproduction of *SAMDC* increased the relative expression levels of *SAMDC* and decreased those of *ACS* in tobacco and *A. thaliana* (Wi et al. 2006, 2014).

In our opinion the prolonged survival and increased salt tolerance of the FvSAMDC lines can be attributed to the higher level of polyamines, while in the FvSAMS lines elevated lignin and polyamines contents together were among the contributing factors.

We investigated the subcellular localization of the proteins encoded by *FvSAMS::sGFP* and *FvSAMDC::sGFP*. The *FvSAMS::sGFP* exhibited nuclear, nucleolar and cytoplasmic (near to the plasmalemma), plastid membrane localization in stable transformants (Fig. 8c). Previous studies reported that the *SAMS* is considered to be an enzyme with cytosolic localization in plants (Schröder et al. 1997; Ravel et al. 1998; Hanson and Roje 2001), whereas in mammals it was found to show nucleocytoplasmic distribution (Reytor et al. 2009). Reytor et al. (2009) reported that the nuclear accumulation of MAT (methionine adenosyltransferase = *SAMS* in plant) showed positive correlations with the trimethylation of the histone H3K27. *FvSAMDC::sGFP* showed weak nuclear and homogeneous cytoplasmic distribution (Fig. 9a). In former studies *SAMDC* activities were found in the chloroplasts, mitochondria and cytosol of

plants (Yamanoha and Cohen 1985; Torrigiani et al. 1986), while only cytoplasmic localization was detected in animals (Gritli-Linde et al. 1995). Since we detected no chloroplast or mitochondrial *sGFP* signals, the amino acid sequence of *FvSAMDC* was examined bioinformatically. According to application, prediction of the probability of *FvSAMDC* having chloroplast, mitochondrial and other localization was found to be 7%, 9% and 80%, respectively.

In the case of both constructs, endoplasmic reticulum subcellular localization was observed during transient expression, but no similar signals were detected in the FvSAMS and FvSAMDC stable transformants (Figs. S1, S2). We assumed therefore that these signals could be interpreted as a response to the physical and biotic stresses caused by the infiltration procedure. This phenomenon cannot be adequately explained by our current data and requires further investigations, but both biotic and abiotic stresses can cause the accumulation of unfolded proteins, which interact with the specific sensor proteins of the ER membrane. The response to the unfolded proteins (UPR—unfolded protein response) is a conserved eukaryotic stress reaction, and it was the unfolded protein ER-associated degradation (ERAD) that we presumably observed (Walter and Ron 2011).

In our experiments the *FvSAMS::sGFP* protein was localized to the nucleolus, an observation which has not been reported previously (Fig. 8a, b). Reytor et al. (2009) found no nucleolar localization of the MAT proteins. With the exception of FC (Fibrillar Center) shown in Fig. 8a ii, the *FvSAMS::sGFP* is localized either in DFC (Dense Fibrillar Component) or in GC (Granular Component) or in both nucleolar components, which take part in the biogenesis of ribosomes. DFC contains the protein fibrillarin (Sirri et al. 2008), which plays a role in the processing of rRNA. Furthermore, an MTase region (Ado-Met-dependent methyltransferase) was identified in the *N. benthamiana* Fibrillarin2 protein (*NbFib2*), which contained SAM binding motives and localized to the nucleolus (Zheng et al. 2016). Therefore, the nucleolar localization of *FvSAMS::sGFP* suggests that it plays a role in ribosome synthesis. The fact that the FvSAMS sequences contain no nucleolar localization signals makes it probable that there is an intermediate interaction required for the nucleolar localization of *FvSAMS::sGFP* proteins, but this phenomenon requires further investigations. Previous studies reported that SAM is delivered into plastids by specific SAM transporters (Ferro et al. 2002; Palmieri et al. 2006), where SAM is required to methylation of DNA, RNA and proteins (Montasser-Kouhsari et al. 1978; Block et al. 2002). According to our results the *FvSAMS::sGFP* showed nuclear, nucleolar and cytoplasmic (near to the plasmalemma), plastid membrane distribution, therefore SAM is assumed to be produced in situ for numerous biochemical reactions (e.g. ribosome biosynthesis, methylation of DNA, RNA, proteins in nucleus and plastid; lignin biosynthesis).



Our results showed that in stable transformants the subcellular localization of the *FvSAMS::sGFP* protein was displaced in the direction of the cytoplasm (near to the plasmalemma and plastid membrane) from the nucleus in response to stress, while the quantity of *FvSAMDC::sGFP* protein showed a parallel increase in both cellular compartments (nucleus, cytoplasm) (Fig. 9b). Several nuclear proteins carry both NLS and NES signals, which control their transport between the cell nucleus and the cytoplasm. The presence of putative bipartite nuclear localization and nuclear export signals in both *FvSAMS* and *FvSAMDC* is in agreement with the nuclear and cytoplasmic localization of both enzymes, though the fictionality of these signals remain to be demonstrated experimentally.

We could randomly detect *FvSAMDC::sGFP* fusion proteins only in a few cases from several dozens of preparations, which can be due to the short half life time of the SAMDC (Pegg 1986), but it could be observed that the *FvSAMDC::sGFP* showed distinctive nuclear, cytoplasmic and nuclear-cytoplasmic localization concurrently in the stable transformants (Fig. 10a). The fact that it showed nuclear and cytoplasmic localization separately and also simultaneously can be explained by the differential autocatalytic activation of the proenzyme SAMDC in the different cellular compartments as well as by the unidirectional dislocation of the enzyme. However, we were not able to identify whether the direction of its movement is cytoplasm → nucleus or nucleus → cytoplasm. The dual localization of the *FvSAMDC::sGFP* is also supported by an earlier study (Belda-Palazón et al. 2012) in which it was described that the spermidine synthase showed nuclear and cytoplasmic localization, whereas the spermine synthase had only cytoplasmic localization. Belda-Palazón et al. (2012) also observed that in the presence of exogenic spermidine synthase, the cytoplasmic localization of spermine synthase showed a displacement towards the nucleus, which suggests that the synthesis of spermidine and spermine is a complex process. Since SAMDC produces dcSAM, which serves as a substrate for both the spermidine and spermine synthases by providing them with aminopropyl group, the synthesis of SAMDC in an inactive form, its strict transcriptional and translational regulation as well as its short half-life can account for its dual localization due to the complexity of the process.

We also observed that the amount of detectable *FvSAMS::sGFP* protein showed a decreasing tendency from the younger leaves towards the older ones but higher *FvSAMS* mRNA rates were measured in the older leaves in spite of the lower levels of detectable *FvSAMS::sGFP* protein. Finally, *FvSAMS::sGFP* fusion proteins were only detected in the guard cells of older leaves (Fig. 10b–d), therefore we suppose that the SAMS enzyme has an important role to play in the regulation of the stomatal functions,

such as cellular respiration, photosynthetic gas exchange and evaporation. Similar pattern was obtained in tobacco plants overexpressing *AtSAMS1* by Boerjan et al. (1994), namely that *AtSAMS1* mRNA accumulation grew from top to bottom but the activity of *AtSAMS1* enzyme showed a reverse correlation to the amount of mRNA. Later it was proven that *AtSAMS1* is inhibited by nitric oxide (NO). Structural analysis of *AtSAMS1* showed that the Cys-114 is flanked with amino acids promoting S-nitrosylation. We found that the amino acid sequence of SAMS contained arginine (R) at the site of Cys-114 (Fig. 11a). The inhibitory effect of S-Nitrosoglutathione (GSNO) drastically decreased when Cys-114 was replaced by arginine (Lindermayr et al. 2006). Earlier studies focused on the reduction in the activity of enzyme SAMS by S-nitrosylation (Avila et al. 1997; Lindermayr et al. 2006), while other publications discussed the phosphorylation of Thr-342 by Protein kinase C (PKC), which decreased the enzyme activity of SAMS (Pajares et al. 1994) as well as the predicted phosphorylation of Thr, Ser, Thr-112 and Ser-271 in *FvSAMS* (Fig. 11b), which is equivalent to the S/TXK/R (Woodgett et al. 1986) and TXRX (Pajares et al. 1994) recognition sequences preferred by PKC (in the case of *FvSAMS* the TKRP and SGK). Therefore, it is possible that we assume that the phosphorylation of Thr-112 and Ser-271 play a role in the inhibition of enzyme *FvSAMS* by PKC, but we currently do not have evidence for this possibility.

According to Reytor et al. (2009) the subcellular localization of the enzyme SAMS is determined by the structure of its C-terminal domain, which makes the involvement of Lys-335, 360, 364 acetylation and Lys-387 SUMOylation in the regulation of subcellular localization of *FvSAMS* probable (Fig. 11c). The results of earlier studies support this hypothesis since the SUMOylation of NLS of the human enzyme SAE resulted in its nuclear accumulation (Truong et al. 2012) and the acetylation of the NLS of the human RhoA GEF Net1A increased its cytoplasmic accumulation (Song et al. 2015). We have no data available with regard to the post-translational modifications determining the subcellular localization of the enzyme *FvSAMDC* but based on predicted data the phosphorylation, acetylation, S-nitrosylation and SUMOylation of the NLSs can play a role in the process (Fig. 11d), since numerous published data provided evidence supporting the role of NLS phosphorylation, acetylation, S-nitrosylation, SUMOylation in the subcellular localization of enzymes (Harreman et al. 2004; Hara et al. 2005; Truong et al. 2012; Song et al. 2015).

**Acknowledgements** Open access funding provided by Szent István University (SZIE). This work was supported by grants from the Hungarian Scientific Research Fund (OTKA 101195) and Higher Education Institutional Excellence Program (20430-3/2018/FEKUT-STRAT) awarded by the Ministry of Human Capacities within the

framework of plant breeding and plant protection researches of Szent István University, 2017-1.3.1-VKE-2017-0030 and the EFOP-3.6.3-VEKOP-16-2017-00008 project (co-financed by the European Union and the European Social Fund).

**Author contributions** The authors performed the following tasks: LK—designed the research, performed research, analyzed data, wrote the paper; AM—performed research, analyzed data; ASZ—performed research, analyzed data; SF—performed research; FS—performed research; KP—designed the research; EK—designed the research, analyzed data, wrote the paper.

## Compliance with ethical standards

**Conflict of interest** The authors declare no conflict of interest.

**Open Access** This article is licensed under a Creative Commons Attribution 4.0 International License, which permits use, sharing, adaptation, distribution and reproduction in any medium or format, as long as you give appropriate credit to the original author(s) and the source, provide a link to the Creative Commons licence, and indicate if changes were made. The images or other third party material in this article are included in the article's Creative Commons licence, unless indicated otherwise in a credit line to the material. If material is not included in the article's Creative Commons licence and your intended use is not permitted by statutory regulation or exceeds the permitted use, you will need to obtain permission directly from the copyright holder. To view a copy of this licence, visit <http://creativecommons.org/licenses/by/4.0/>.

## References

- Ábrahám E, Hourton-Cabassa C, Szabados L (2010) Methods for determination of proline in plants. In: Sunkar R (ed) Plant stress tolerance, methods in molecular biology. Humana Press, Totowa, pp 317–331
- Avila MA, Mingorance J, Martínez-Chantar ML, Casado M, Martín-Sanz P, Bosca L, Mato JM (1997) Regulation of rat liver S-adenosylmethionine synthetase during septic shock: role of nitric oxide. *Hepatology* 25:391–396
- Azaizeh H, Steudle E (1991) Effects of salinity on water transport of excised maize (*Zea mays* L.) roots. *Plant Physiol* 97:1136–1145
- Belda-Palazón B, Ruiz L, Martí E, Tárraga S, Tiburcio AF, Culiáñez F, Farràs R, Carrasco P, Ferrando A (2012) Aminopropyltransferases involved in polyamine biosynthesis localize preferentially in the nucleus of plant cells. *PLoS ONE* 7:e46907
- Bennett EM, Ekstrom JL, Pegg AE, Ealick SE (2002) Monomeric S-adenosylmethionine decarboxylase from plants provides an alternative to putrescine stimulation. *Biochemistry* 41:14509–14517
- Biswas MS, Mano J (2015) Lipid peroxide-derived short-chain carbonyls mediate H<sub>2</sub>O<sub>2</sub>-induced and NaCl-induced programmed cell death in plants. *Plant Physiol* 168:885–898
- Block MA, Tewari AK, Albrieux C, Marechal E, Joyard J (2002) The plant S-adenosyl-L-methionine: Mg-protoporphyrin IX methyltransferase is located in both envelope and thylakoid chloroplast membranes. *Eur J Biochem* 269:240–248
- Boerjan W, Bauw G, Montagu MV, Inzé D (1994) Distinct phenotypes generated by overexpression and suppression of S-adenosyl-L-methionine synthetase reveal developmental patterns of gene silencing in tobacco. *Plant Cell* 6:1401–1414
- Cantoni GL (1975) Biological methylation: selected aspects. *Annu Rev Biochem* 44:435–451
- Cheng L, Zou Y, Ding S, Zhang J, Yu X, Cao J, Lu G (2009) Polyamine accumulation in transgenic tomato enhances the tolerance to high temperature stress. *J Integr Plant Biol* 51:489–499
- Chinnusamy V, Zhu J, Zhu JK (2006) Salt stress signaling and mechanisms of plant salt tolerance. *Genet Eng* 27:141–177
- Clemente T (2006) *Nicotiana tabacum*, *Nicotiana benthamiana*. *Methods Mol Biol* 343:143–154
- Cruz RT, Jordan WR, Drew MC (1992) Structural changes and associated reduction of hydraulic conductance in roots of *Sorghum bicolor* L. following exposure to water deficit. *Plant Physiol* 99:203–212
- Cvikrová M, Gemperlová L, Dobrá J, Martincová O, Prášil IT, Gubis J, Vanková R (2012) Effect of heat stress on polyamine metabolism in proline-over-producing tobacco plants. *Plant Sci* 182:49–58
- Emanuelsson O, Brunak S, von Heijne G, Nielsen H (2007) Locating proteins in the cell using TargetP, SignalP, and related tools. *Nat Protoc* 2:953–971
- Ferro M, Salvi D, Riviere-Rolland H, Verdat T, Seigneurin-Berny D, Grunwald D, Garin J, Joyard J, Rolland N (2002) Integral membrane proteins of the chloroplast envelope: identification and subcellular localization of new transporters. *Proc Natl Acad Sci USA* 99:11487–11492
- Fontecave M, Atta M, Mulliez E (2004) S-adenosylmethionine: nothing goes to waste. *Trends Biochem Sci* 29:243–249
- Franceschetti M, Hanfrey C, Scaramagli S, Torrigiani P, Bagni N, Burtin D, Michael AJ (2001) Characterization of monocot and dicot plant S-adenosyl-L-methionine decarboxylase gene families including identification in the mRNA of a highly conserved pair of upstream overlapping open reading frames. *Biochem J* 353:403–409
- Ge C, Cui X, Wang Y, Hu Y, Fu Z, Zhang D, Cheng Z, Li J (2006) *BUD2*, encoding an S-adenosylmethionine decarboxylase, is required for *Arabidopsis* growth and development. *Cell Res* 16:446–456
- Gnad F, Gunawardena J, Mann M (2011) PHOSIDA 2011: the posttranslational modification database. *Nucleic Acids Res* 39:253–260
- Gong B, Xiu L, Vandenlangenberg KM, Dan W, Shasha S, Min W, Yan L, Fengujan Y, Qinghua S, Xiufeng W (2014) Overexpression of S-adenosyl-L-methionine synthetase increased tomato tolerance to alkali stress through polyamine metabolism. *Plant Biotechnol J* 12:694–708
- Gritli-Linde A, Holm I, Linde A (1995) Localization of S-adenosylmethionine decarboxylase in murine tissues by immunohistochemistry. *Eur J Oral Sci* 103:133–140
- Guo Z, Tan J, Zhuo C, Wang C, Xiang B, Wang Z (2014) Abscisic acid, H<sub>2</sub>O<sub>2</sub> and nitric oxide interactions mediated cold-induced S-adenosylmethionine synthetase in *Medicago sativa* subsp. *falcata* that confers cold tolerance through up-regulating polyamine oxidation. *Plant Biotechnol J* 12:601–612
- Hanson AD, Roje S (2001) One-carbon metabolism in higher plants. *Annu Rev Plant Phys* 52:119–137
- Hara MR, Agrawal N, Kim SF, Cascio MB, Fujimuro M, Ozeki Y, Takahashi M, Cheah JH, Tankou SK, Hester LD, Ferris CD, Hayward SD, Snyder SH, Sawa A (2005) S-nitrosylated GAPDH initiates apoptotic cell death by nuclear translocation following Siah1 binding. *Nat Cell Biol* 7:665–674
- Harreman MT, Kline TM, Milford HG, Harben MB, Hode AE, Corbett AH (2004) Regulation of nuclear import by phosphorylation adjacent to nuclear localization signals. *J Biol Chem* 279:20613–20621
- Hu WW, Gong H, Pua EC (2005) The pivotal roles of plant S-adenosylmethionine decarboxylase 5' untranslated leader sequence

- in regulation of gene expression at the transcriptional and post-transcriptional levels. *Plant Physiol* 138:276–286
- Hu WW, Gong H, Pua EC (2006) Modulation of *SAMDC* expression in *Arabidopsis thaliana* alters *in vitro* shoot organogenesis. *Physiol Plant* 128:740–750
- Jang SJ, Wi SJ, Choi YJ, An G, Park KY (2012) Increased polyamine biosynthesis enhances stress tolerance by preventing the accumulation of reactive oxygen species: T-DNA mutational analysis of *Oryza sativa* lysine decarboxylase-like protein 1. *Mol Cells* 34:251–262
- Kamal AH, Cho K, Kim DE, Uozumi N, Chung KY, Lee SY, Choi JS, Cho SW, Shin CS, Woo SH (2012) Changes in physiology and protein abundance in salt-stressed wheat chloroplasts. *Mol Biol Rep* 39:9059–9074
- Kim SH, Kim SH, Palaniyandi SA, Yang SH, Suh JW (2015) Expression of potato S-adenosyl-L-methionine synthase (*SbSAMS*) gene altered developmental characteristics and stress responses in transgenic *Arabidopsis* plants. *Plant Physiol Biochem* 87:84–91
- Kosugi S, Hasebe M, Tomita M, Yanagawa H (2009) Systematic identification of yeast cell cycle-dependent nucleocytoplasmic shuttling proteins by prediction of composite motifs. *Proc Natl Acad Sci USA* 106:10171–10176
- Kumar D, Yusuf MA, Singh P, Sardar M, Sarin NB (2014) Histochemical detection of superoxide and H<sub>2</sub>O<sub>2</sub> accumulation in *Brassica juncea* seedlings. *Bio-Protoc* 4:1108
- Kusano T, Suzuki H (2015) Polyamine homeostasis in plants: the role(s) of evolutionarily conserved upstream ORFs. In: Kusano T, Suzuki H (eds) *Polyamines: a universal molecular nexus for growth, survival, and specialized metabolism*. Springer, Tokyo, pp 111–118
- Kusano T, Berberich T, Tateda C, Takahashi Y (2008) Polyamines: essential factors for growth and survival. *Planta* 228:367–381
- La Cour T, Kiemer L, Mølgaard A, Gupta R, Skriver K, Brunak S (2004) Analysis and prediction of leucine-rich nuclear export signals. *Protein Eng Des Sel* 17:527–536
- Langebartels C, Kerner K, Leonardi S, Schraudner M, Trost M, Heller W, Sandermann H Jr (1991) Biochemical plant responses to ozone. I. Differential induction of polyamine and ethylene biosynthesis of tobacco. *Plant Physiol* 95:882–889
- Li X (2011) Infiltration of *Nicotiana benthamiana* protocol for transient expression via *Agrobacterium*. *Bio-Protoc* 101:e95
- Li C, Jiao J, Wang G (2004) The important roles of reactive oxygen species in the relationship between ethylene and polyamines in leaves of spring wheat seedlings under root osmotic stress. *Plant Sci* 166:303–315
- Lindermayr C, Saalbach G, Bahnweg G, Durner J (2006) Differential inhibition of *Arabidopsis* methionine adenosyltransferases by protein S-nitrosylation. *J Biol Chem* 281:4285–4291
- Liu JH, Kitashiba H, Wang J, Ban Y, Moriguchi T (2007) Polyamines and their ability to provide environmental stress tolerance to plants. *Plant Biotechnol* 24:117–126
- Liu JH, Inoue H, Moriguchi T (2008) Salt stress-mediated changes in free polyamine titers and expression of genes responsible for polyamine biosynthesis of apple *in vitro* shoots. *Environ Exp Bot* 62:28–35
- Ma C, Wang Y, Gum D, Nan J, Chen S, Li H (2017) Overexpression of S-adenosyl-L-methionine synthetase 2 from sugar beet M14 increased *Arabidopsis* tolerance to salt and oxidative stress. *Int J Mol Sci* 18:847
- Mahajan S, Tuteja N (2005) Cold, salinity and drought stresses: an overview. *Arch Biochem Biophys* 444:139–158
- McCurdy RD, McGrath JJ, Mackay-Sim A (2008) Validation of the comparative quantification method of real-time PCR analysis and a cautionary tale of housekeeping gene selection. *Gene Ther Mol Biol* 12:15–24
- Mellidou I, Moschou PN, Ioannidis NE, Pankou C, Gemes K, Valassakis C, Andronis EA, Beris D, Haralampidis K, Roussis A, Karamanoli A, Matsi T, Kotzabasis K, Constantinidou HI, Roubelakis-Angelakis KA (2016) Silencing S-adenosyl-L-methionine decarboxylase (*SAMDC*) in *Nicotiana tabacum* points at a polyamine-dependent trade-off between growth and tolerance responses. *Front Plant Sci* 7:379
- Merali S, Clarkson AB Jr (2004) S-adenosylmethionine and pneumocystis. *FEMS Microbiol Lett* 237:179–186
- Mignolet-Spruyt L, Xu E, Idänheimo N, Hoerberichts FA, Mühlenbock P, Brosché M, Van Breusegem F, Kangasjärvi J (2016) Spreading the news: subcellular and organellar reactive oxygen species production and signalling. *J Exp Bot* 67:3831–3844
- Montasser-Kouhsari S, Keith G, Weil GH (1978) Methylation of yeast tRNAPhe by enzymes from cytoplasm, chloroplasts and mitochondria of *Phaseolus vulgaris*. *Biochim Biophys Acta* 521:576–583
- Moreira-Vilar FC, de Cassia Siqueira-Soares R, Finger-Teixeira A, de Oliveira DM, Ferro AP, da Rocha GJ, Ferrarese MD, dos Santos WD, Ferrarese-Filho O (2014) The acetyl bromide method is faster, simpler and presents best recovery of lignin in different herbaceous tissues than Klason and thioglycolic acid methods. *PLoS ONE* 9:e110000
- Mostofa MG, Yoshida N, Fujita M (2014) Spermidine pretreatment enhances heat tolerance in rice seedlings through modulating antioxidative and glyoxalase systems. *Plant Growth Regul* 73:31–44
- Müller M, Munné-Bosch S (2015) Ethylene response factors: a key regulatory hub in hormone and stress signaling. *Plant Physiol* 169:32–41
- Nambeesan S, AbuQamar S, Laluk K, Mattoo AK, Mickelbart MV, Ferruzzi MG, Mengiste T, Handa AK (2012) Polyamines attenuate ethylene-mediated defense responses to abrogate resistance to *Botrytis cinerea* in tomato. *Plant Physiol* 158:1034–1045
- Németh M, Janda T, Horváth E, Páldi E, Szalai G (2002) Exogenous salicylic acid increases polyamine content but may decrease drought tolerance in maize. *Plant Sci* 162:569–574
- Neves GYS, Marchiosi R, Ferrarese MLL, Siqueira-Soares RC, Ferrarese-Filho O (2010) Root growth inhibition and lignification induced by salt stress in soybean. *J Agron Crop Sci* 196:467–473
- Pajares MA, Duran C, Corrales F, Mato JM (1994) Protein kinase C phosphorylation of rat liver S-adenosylmethionine synthetase: dissociation and production of an active monomer. *Biochem J* 303:949–955
- Palmieri L, Arrigoni R, Blanco E, Carrari F, Zanor MI, Studart-Guimaraes C, Fernie AR, Palmieri F (2006) Molecular identification of an *Arabidopsis* S-Adenosylmethionine transporter. analysis of organ distribution, bacterial expression, reconstitution into liposomes, and functional characterization. *Plant Physiol* 142:855–865
- Pegg AE (1986) Recent advances in the biochemistry of polyamines of eukaryotes. *Biochem J* 234:249–262
- Peng J, Li Z, Wen X, Li W, Shi H, Yang L, Zhu H, Guo H (2014) Salt-induced stabilization of EIN3/EIL1 confers salinity tolerance by deterring ROS accumulation in *Arabidopsis*. *PLoS Genet* 10:e1004664
- Peremarti A, Bassie L, Christou P, Capell T (2009) Spermine facilitates recovery from drought but does not confer drought tolerance in transgenic rice plants expressing *Datura stramonium* S-adenosylmethionine decarboxylase. *Plant Mol Biol* 70:253–264
- Porra RJ, Thompson WA, Kriedemann PE (1989) Determination of accurate extinction coefficients and simultaneous equations

- for assaying chlorophylls *a* and *b* extracted with four different solvents: verification of the concentration of chlorophyll standards by atomic absorption spectroscopy. *Biochim Biophys Acta* 975:384–394
- Pulla RK, Kim YJ, Parvin S, Shim JS, Lee JH, Kim YJ, In JG, Senthil KS, Yang DC (2009) Isolation of S-adenosyl-L-methionine synthetase gene from *Panax ginseng* C. A. Meyer and analysis of its response to abiotic stresses. *Physiol Mol Biol Plants* 15:267–275
- Qi YC, Wang FF, Zhang H, Liu WQ (2010) Overexpression of *Suaeda salsa* S-adenosylmethionine synthetase gene promotes salt tolerance in transgenic tobacco. *Acta Physiol Plant* 32:263–269
- Ravanel S, Gakière B, Job D, Douce R (1998) The specific features of methionine biosynthesis and metabolism in plants. *Proc Natl Acad Sci USA* 95:7805–7812
- Reytor E, Pérez-Miguelsanz J, Alvarez L, Pérez-Sala D, Pajares MA (2009) Conformational signals in the C-terminal domain of methionine adenosyltransferase I/III determine its nucleocytoplasmic distribution. *FASEB J* 23:3347–3360
- Rizhsky L, Hallak-Herr E, Van Breusegem F, Rachmilevich S, Barr JE, Rodermel S, Inzé D, Mittler R (2002) Double antisense plants lacking ascorbate peroxidase and catalase are less sensitive to oxidative stress than single antisense plants lacking ascorbate peroxidase or catalase. *Plant J* 32:329–342
- Roeder S, Dreschler K, Wirtz M, Cristescu SM, van Harren FJ, Hell R, Piechulla B (2009) SAM levels, gene expression of SAM synthase, methionine synthase and ACC oxidase, and ethylene emission from *N. suaveolens* flowers. *Plant Mol Biol* 70:535–546
- Romero FM, Maiale SJ, Rossi FR, Marina M, Ruíz OA (2018) Gárriz A (2018) Polyamine metabolism responses to biotic and abiotic stress. In: Alcazar R, Tiburcio AF (eds) Polyamines: methods and protocols, methods in molecular biology. Humana Press, New York, pp 37–49
- Roy M, Wu R (2002) Overexpression of S-adenosylmethionine decarboxylase gene in rice increases polyamine level and enhances sodium chloride-stress tolerance. *Plant Sci* 163:987–992
- Saha J, Brauer EK, Sengupta A, Popescu SC, Gupta K, Gupta B (2015) Polyamines as redox homeostasis regulators during salt stress in plants. *Front Environ Sci* 3:1–13
- Sánchez-Aguayo I, Rodríguez-Galán JM, García R, Torreblanca J, Pardo JM (2004) Salt stress enhances xylem development and expression of S-adenosyl-L-methionine synthase in lignifying tissues of tomato plants. *Planta* 220:278–285
- Schneider CA, Rasband WS, Eliceiri KW (2012) NIH Image to ImageJ: 25 years of image analysis. *Nat Methods* 9:671–675
- Schröder G, Eichel J, Breining S, Schröder J (1997) Three differentially expressed S-adenosylmethionine synthetase from *Catharantus roseus*: molecular and functional characterization. *Plant Mol Biol* 33:211–222
- Scott MS, Troshin PV, Barton GJ (2011) NoD: a Nucleolar localization sequence detector for eukaryotic and viral proteins. *BMC Bioinform* 12:317
- Shen B, Li C, Tarczynski MC (2002) High free-methionine and decreased lignin content result from a mutation in the *Arabidopsis* S-adenosyl-L-methionine synthetase 3 gene. *Plant J* 29:371–380
- Shen X, Wang Z, Song X, Xu J, Jiang C, Zhao Y, Ma C, Zhang H (2014) Transcriptomic profiling revealed an important role of cell wall remodeling and ethylene signaling pathway during salt acclimation in *Arabidopsis*. *Plant Mol Biol* 86:303–317
- Shi J, Fu XZ, Peng T, Huang XS, Fan QJ, Liu JH (2010) Spermine pretreatment confers dehydration tolerance of citrus *in vitro* plants via modulation of antioxidative capacity and stomatal response. *Tree Physiol* 30:914–922
- Simon-Sarkadi L, Kocsy G, Várhegyi Á, Galiba G, de Ronde JA (2006) Effect of drought stress at supraoptimal temperature on polyamine concentrations in transgenic soybean with increased proline levels. *Z Naturforsch C* 61:833–839
- Sirri V, Urcuqui-Inchima S, Roussel P, Hernandez-Verdun D (2008) Nucleolus: the fascinating nuclear body. *Histochem Cell Biol* 129:13–31
- Smith MA, Davies PJ (1985) Separation and quantitation of polyamines in plant tissue by high performance liquid chromatography of their dansyl derivatives. *Plant Physiol* 78:89–91
- Song EH, Oh W, Ulu A, Carr HS, Zuo Y, Frost JA (2015) Acetylation of the RhoA GEF Net1A controls its subcellular localization and activity. *J Cell Sci* 128:913–922
- Tao JJ, Chen HW, Ma B, Zhang WK, Chen SY, Zhang JS (2015) The role of ethylene in plants under salinity stress. *Front Plant Sci* 6:1–12
- Torrighiani P, Serafini-Fracassini D, Biondi S, Bagni N (1986) Evidence for the subcellular localization of polyamines and their biosynthetic enzymes in plant cells. *J Plant Physiol* 124:23–29
- Torrighiani P, Scaramagli S, Ziosi V, Mayer M, Biondi S (2005) Expression of an antisense *Datura stramonium* S-adenosylmethionine decarboxylase cDNA in tobacco: changes in enzyme activity, putrescine-spermidine ratio, rhizogenic potential, and response to methyl jasmonate. *J Plant Physiol* 162:559–571
- Truong K, Lee TD, Li B, Chen Y (2012) Sumoylation of SAE2 C terminus regulates SAE nuclear localization. *J Biol Chem* 287:42611–42619
- Urano K, Yoshida Y, Nanjo T, Igarashi Y, Seki M, Sekiguchi F, Yamaguchi-Shinozaki K, Shinozaki K (2003) Characterization of *Arabidopsis* genes involved in biosynthesis of polyamines in abiotic stress responses and developmental stages. *Plant Cell Environ* 26:1917–1926
- Velikova V, Yordanov I, Edreva A (2000) Oxidative stress and some antioxidant system in acid rain treated bean plants: protective role of exogenous polyamines. *Plant Sci* 151:59–66
- Waie B, Rajam MV (2003) Effect of increased polyamine biosynthesis on stress responses in transgenic tobacco by introduction of human S-adenosylmethionine gene. *Plant Sci* 164:727–734
- Walter P, Ron D (2011) The unfolded protein response: from stress pathway to homeostatic regulation. *Science* 334:1081–1086
- Warton K, Foster NC, Gold WA, Stanley KK (2004) A novel gene family induced by acute inflammation in endothelial cells. *Gene* 342:85–89
- Wen XP, Ban Y, Inoue H, Matsuda N, Kita M, Moriguchi T (2011) Antisense inhibition of a spermidine synthase gene highlights the role of polyamine for stress alleviation in pear shoots subjected to salinity and cadmium. *Environ Exp Bot* 72:157–166
- Wi SJ, Kim WT, Park KY (2006) Overexpression of carnation S-adenosylmethionine decarboxylase gene generates a broad spectrum tolerance to abiotic stresses in transgenic tobacco plants. *Plant Cell Rep* 25:1111–1121
- Wi SJ, Kim SJ, Kim WT, Park KY (2014) Constitutive S-adenosylmethionine decarboxylase gene expression increases drought tolerance through inhibition of reactive oxygen species accumulation in *Arabidopsis*. *Planta* 30:30
- Woodgett JR, Gould KL, Hunter T (1986) Substrate specificity of protein kinase C. *Eur J Biochem* 161:177–184
- Xue Y, Liu Z, Gao X, Jin C, Wen L, Yao X, Ren J (2010) GPS-SNO: Computational prediction of protein S-nitrosylation sites with a modified GPS algorithm. *PLoS ONE* 5:e11290
- Yamanoha B, Cohen SS (1985) S-adenosylmethionine decarboxylase and spermidine synthase from Chinese cabbage. *Plant Physiol* 78:784–790
- Yu Y, Jin C, Sun C, Wang J, Ye Y, Zhou W, Lu L, Lin X (2016) Inhibition of ethylene production by putrescine alleviates aluminium-induced root inhibition in wheat plants. *Sci Rep* 6:18888

- Zheng L, Yao J, Gao F, Chen L, Zhang C, Lian L, Xie L, Wu Z, Xie L (2016) The subcellular localization and functional analysis of Fibrillarin2, a nucleolar protein in *Nicotiana benthamiana*. *Biomed Res Int* 2016:2831287
- Zhu JK (2002) Salt and drought stress signal transduction in plants. *Annu Rev Plant Biol* 53:247–273

**Publisher's Note** Springer Nature remains neutral with regard to jurisdictional claims in published maps and institutional affiliations.